RSC Advances

PAPER

View Article Online
View Journal | View Issue

Cite this: *RSC Adv.*, 2026, **16**, 27718

Covalent engineering of a phenanthroline-modified NH_2-MIL-53(Al) MOF for the dual-mode sensing of As^{3+} and Fe^{2+} in complex environmental and dietary matrices

Salhah D. Al-Qahtani,[a] Ghadah M. Al-Senani,[a] Abeer Abdulaziz H. Bukhari,[b] Menier Al-Anazi,[b] Humaira Parveen,[b] Uzma Faridi[c] and M. A. M. El-Afify *[d]

Simultaneous detection of toxic metalloids and transition metals in water systems is crucial for environmental safety and public health. The current work presents the design and fabrication of a novel dual-analyte spectrophotometric sensor, Phen-GA-MIL-53(Al), developed through the covalent post-synthetic modification of an amino-functionalized aluminum-based metal–organic framework NH_2-MIL-53(Al). Sensing architecture was constructed by anchoring 5-amino-1,10-phenanthroline onto the MOF scaffold using glutaraldehyde as a flexible molecular spacer to create a high-density chelating environment within hierarchical pores. XRD, SEM-EDX, and BET studies validated the framework's structure and high surface area 1384 $m^2\ g^{-1}$ after functionalization. Experimental data demonstrated that the sensor had exceptional sensitivity to As^{3+} at pH 4.0 and Fe^{2+} at pH 7.0. Detection of As^{3+} was controlled by a complex system of hydrogen bonding and Lewis acid-base interactions. On the other hand, for Fe^{2+}, there was an observable chromogenic change to "naked-eye" from pale cream to orange-red with a strong MLCT absorption band; the chromogenic transition can be seen by naked-eye and does not need any specialized instrumentation. This makes it suitable for many field-screening applications. Both analytes had fast kinetics and broad linear ranges, with low limits of detection (LOD). 2D-COS and DFT calculations have provided great insights into the sensing mechanism, which is based on a sequential coordination pathway and a large decrease in the HOMO–LUMO energy gap after binding with an analyte. The sensor also has very high selectivity, good storage stability up to six weeks, and excellent reusability using Thiourea and EDTA as stripping agents. Practical tests of Phen-GA-MIL-53(Al) were done by analyzing tap water and dietary supplements that gave recovery rates between 97.27–99.83%, matching well with standard ICP-OES results. This study offers a flexible and field-deployable platform for ultra-trace detection of multi-target pollutants in complicated environmental matrices.

Received 8th April 2026
Accepted 11th May 2026

DOI: 10.1039/d6ra02963a

rsc.li/rsc-advances

1. Introduction

Water resources are the basis for human health, environmental sustainability, and industrial development.[1] Rapid industrialization, urban sprawl, mining activities, and agricultural practices have greatly increased the volume of hazardous contaminants discharged into aquatic systems. Among these pollutants, heavy metals are one of the most persistent and environmentally threatening classes due to their non-biodegradable nature and long-term accumulation with entry into biological food chains.[2] Organic pollutants may degrade; however, metallic contaminants remain chemically stable and gradually accumulate in water bodies, sediments as well as living organisms. It is consequently no surprise that heavy metal aqueous pollution has been described as a global environmental challenge necessitating continuous monitoring coupled with rapid detection strategies.[3] Safe water quality can therefore be ensured through efficient remediation technologies supplemented by reliable sensing platforms for the detection of toxic metal ions at trace concentrations under real environmental conditions.

Heavy metal contamination is very alarming since low concentrations can trigger severe biological and ecological effects.[4] The monitoring system must be sensitive, selective, and

[a]*Department of Chemistry, College of Science, Princess Nourah Bint Abdulrahman University, P.O. Box 84428, Riyadh 11671, Saudi Arabia*
[b]*Department of Chemistry, Faculty of Science, University of Tabuk, Tabuk, 71491, Saudi Arabia*
[c]*Department of Biochemistry, Faculty of Science, University of Tabuk, Tabuk, Saudi Arabia*
[d]*Egyptian Propylene and Polypropylene Company, Port Said 42511, Egypt. E-mail: maher.elafify@yahoo.com*

rapid to avoid the risk of long-term exposure. Traditional environmental monitoring approaches often involve laboratory analyses that are centralized; thus, real-time decision making and early contamination control become limited.[5] As there is an increase in global water stress and industrial effluents become more chemically complex, the need for advanced sensing materials that can perform on-site monitoring has reached a critical level. In this regard, designing smart functional materials with both chemical selectivity and structural stability is a major scientific priority for environmental analytical chemistry.[6]

In the case of metal species that are relevant to the environment, iron and arsenic provide a particularly important yet contrasting case study that brings to light the complexity involved in monitoring aqueous metals.[7] Iron is an essential micronutrient for many biological processes, such as those related to transport of oxygen, enzymatic activities, and cellular metabolism. Naturally occurring forms of iron exist abundantly in any groundwater system, while controlled concentrations should be present for ecological as well as physiological balance. On the other hand, high levels of iron may result in serious environmental hazards and health problems by means of oxidative stress, organ damage, and degradation of water quality through discoloration, taste change plus biofouling effects; elevated concentrations might further elicit secondary contamination processes *via* microbial growth-enhancing redox reactions within aquatic environments.[8] This dual nature makes it necessary for accurate monitoring systems to differentiate between safe and hazardous concentration ranges.

On the other hand, arsenic is one of the most toxic and heavily regulated elements found in water systems.[9] Arsenic contamination mainly comes from geological leaching, mining activities, industrial effluent, and pesticide residues. Chronic exposure to arsenic-contaminated water has been strongly linked with skin lesions, cardiovascular diseases, neurological impairment, and different types of cancer.[10] Arsenic compounds are classified as Group I human carcinogens by IARC; hence there is a great need for reliable detection technologies that can identify arsenic species at ultra-low concentrations.[11] Due to the fact that arsenic toxicity occurs even at trace levels requires continuous environmental monitoring rather than laboratory testing if public health is to be protected. The presence of essential metals like iron together with highly toxic species such as arsenic makes analytical detection more difficult hence high selectivity and discrimination capability are required in sensing materials.[12]

At present, quantitative methods for detecting metal ions in water primarily rely on high-end instruments such as inductively coupled plasma mass spectrometry (ICP-MS), atomic absorption spectroscopy (AAS), and inductively coupled plasma optical emission spectroscopy (ICP-OES).[13] Although these analytical techniques offer high sensitivity and precision, they have several intrinsic drawbacks that limit their use in environmental settings. These methods usually require advanced equipment, trained personnel, high operating costs, and intricate sample preparation steps.[14] In addition, laboratory-based analyses do not allow for real-time monitoring and restrict quick field tests in remote or under-resourced areas. As environmental monitoring increasingly moves toward decentralized and continuous sensing systems, the demand for portable, inexpensive solid-state sensors that can be used for direct *in situ* detection without large infrastructure requirements also grows.[15]

Advanced porous materials have attracted a lot of scientific interest as solid-state sensing platforms, seen as promising alternatives to conventional analysis methods.[16] Among new materials, metal–organic frameworks (MOFs) quickly became popular because of their excellent structural adjustability, large surface area, and controllable chemical properties.[17] MOFs are made up of metal nodes connected by organic linkers to create very ordered porous structures that can be designed at the molecular level for certain sensing uses. Their modular design allows for the exact addition of functional groups that can selectively interact with specific analytes; this makes them very appealing candidates for chemical sensing and environmental monitoring.

Even though these benefits exist, one of the big problems holding back the real use of MOFs in water settings is their tendency to break down when exposed to water.[18] Many MOF designs lose their crystal form or structural strength when kept in water for a long time, making it hard for them to be used in nature. Thus, picking frameworks that can handle water without changing is an important step for building good sensors that work with water.[19] From many families of MOFs, the aluminum-based framework NH_2-MIL-53 has come out as a very exciting option because it has awesome chemical stability, a flexible breathing structure, and strong resistance to hydrolysis under aqueous conditions. The presence of amino functional groups within the organic linker also provides reactive sites that allow for chemical modification and enhanced interaction with metal ions. These features make NH_2-MIL-53 a perfect base for strong sensing platforms that can function in real water systems.[20]

Post-synthetic modification has emerged as a powerful tool for enhancing the selectivity and performance of sensors by engineering the functionality of metal–organic frameworks without altering their underlying crystal structures.[21] It enables the post-formation introduction of specific recognition sites, maintaining crystallinity while increasing chemical responsiveness. Among the various strategies used in post-synthetic modification, one of the most versatile is the reaction of amino functionalized frameworks with aldehyde-containing molecules *via* Schiff base condensation.[22] This modification introduces imine (–C=N–) coordination sites which can provide very strong chelation interactions with metal ions to achieve high selectivity towards specific contaminants. The functionalization through Schiff base not only increases binding affinity but also changes electronic properties within the framework that can enhance sensing signals and improve detection sensitivity.[23] The combination of hydrolytically stable metal–organic frameworks with Schiff base functional groups presents an advanced materials design approach toward next-generation solid-state sensors.[24] Such systems, by virtue of their structural robustness and tunable porosity combined with

chemically engineered recognition sites, promise a significant step forward in selective detection of environmentally relevant metal ions such as iron and arsenic in aqueous media. More importantly, they enable the shift from traditional laboratory-based analyses to portable sensing technologies for actual real-time environmental monitoring.[25]

In our current research paper, we report a novel dual-analyte sensor – Phen-GA-MIL-53(Al) – to detect both the analytes simultaneously. To improve the accessibility of the chelating sites of low surface area metal organic framework MIL-53(Al) towards the chelating agent (5-amino-1,10-phenanthroline), a flexible spacer (glutaraldehyde) was effectively used. This highly soluble in water organic sensor readily crosslinking in the presence of the amine functional groups of the phenanthroline by Schiff base formation improves the accessibility of these sites. Subsequent to this the synthesis of the dual-analyte sensor material results in the rapid formation of stable and highly sensitive complexes $[Fe(phen)_3]^{2+}$ on surface of the sensor by post-synthetic metallo-organotopic approach. Such surface confined stable photoluminescent complex on MOF surface enhances the detection of Fe^{2+}. The detection of arsenic from waste water sample is very critical due to presence of hazardous chemical which are not only harmful for water pollution but also for metals like calcium due to their bio-accumulation property. The detection is made possible by introducing novel methodology of employing same sensor material for different analytes the MIL-53(Al) surface with similar sized d-p orbital of As^{3+} due to van der Waals forces of attraction which enhances the spectral overlap of motion in the cadmium chromophore of the sensor material. 2D-COS has been performed to confirm the anti-correlation between the analytes introduced. The utilization of the sensor material to detect two analytes (As^{3+} and Fe^{2+}) has made this sensor advantageous over the other conventional spectrometric sensors. The sensor material has been further applied in the analysis of environmental water samples and dietary supplements by conducting various performing a range of tests (selectivity, life time and sensor fabrication). The results obtained were accurate and matched with the values from the standard method ICP-OES. DFT calculations were performed to theorize the anti-formation mechanism and stability of the sensor when two analytes were introduced.

2. Material and methods

2.1 Materials

All the chemical reagents and solvents used were of analytical grade and were used as they came without any further purification unless otherwise stated. Aluminum chloride hexahydrate ($AlCl_3 \cdot 6H_2O$ 98%) and 2-aminoterephthalic acid (NH_2-BDC, 99%) from Sigma-Aldrich were taken to be the metal precursor and organic linker, respectively, in the synthesis of NH_2-MIL-53(Al) MOF. The main solvents for solvothermal synthesis and then washing steps were *N*,*N*-dimethylformamide (DMF, 99.8%), absolute ethanol (CH_3CH_2OH), and deionized water with a resistance of 18.2 MΩ·cm. In the post-synthetic modification of the MOF scaffold, glutaraldehyde (GA, 25 wt% in water) served as the dialdehyde cross-linker, while 5-amino-1,10-phenanthroline (97%) acted as the chromogenic ligand; both were sourced from Merck. Standard stock solutions of the target analytes were prepared at a concentration of 1000 mg L^{-1} by dissolving high-purity salts of sodium arsenite and ferrous sulfate heptahydrate in DI water. To keep Fe^{2+} from oxidizing to Fe^{3+}, the iron stock solutions were made fresh every day and stabilized with a small amount of 0.1 M H_2SO_4. Interference studies used salts of Na^+, K^+, Ca^{2+}, Mg^{2+}, Cu^{2+}, Ni^{2+}, Pb^{2+}, Co^{2+}, Zn^{2+}, Hg^{2+}, Cl^-, NO_3^-, SO_4^{2-} and PO_4^{3-}. The pH was adjusted from 2.0 to 10.0 with buffer systems: HCl/KCl for the acidic medium, CH_3COONa/CH_3COOH for the weakly acidic medium, and Na_2HPO_4/NaOH for the neutral to alkaline medium.

2.2 Synthesis of NH_2-MIL-53(Al)

Amino-MIL-53(Al) frameworks were synthesized by following the procedure described in the literature.[26] The synthesis was carried out at room temperature in an aqueous medium. Typically, 0.543 g of 2-aminoterephthalic acid was dissolved in 30 mL of distilled water and sonicated for 30 minutes. To this solution, 0.724 g of $AlCl_3 \cdot 6H_2O$ was added, and the resulting mixture was sonicated for another 30 minutes (Scheme 1). The resulting solution was transferred into a 50 mL Teflon-lined autoclave and heated at 150 °C for six hours. The yellow precipitate formed was centrifuged to remove any unreacted materials and washed three times with deionized water and DMF before being allowed to cool to room temperature. Subsequently, the solid product was activated by stirring it in anhydrous methanol for 24 hours, followed by drying under vacuum at 70 °C for twelve hours.

2.3 Synthesis of Phen-GA-MIL-53(Al) sensor

The 5-amino-1,10-phenanthroline ligand was covalently attached to the MOF framework *via* a two-step post-synthetic modification using glutaraldehyde as a cross-linking spacer. Activated NH_2-MIL-53(Al) 0.5 g was dispersed in 30 mL of ethanol that contained 2 mL of glutaraldehyde. The mixture was stirred at room temperature for 6 hours. This step allowed the formation of an imine bond between the amino groups of the MOF and one aldehyde group of the glutaraldehyde, thereby generating a free pendant aldehyde group for further reaction. A solution of 0.1 g of 5-amino-1,10-phenanthroline in 10 mL ethanol was added dropwise to the above mixture. The resulting reaction mixture was heated at 70 °C and kept under reflux for 12 hours in order to complete the Schiff base condensation. The material that was functionalized, referred to as Phen-GA-MIL-53(Al), was separated through centrifugation, thoroughly washed with ethanol and deionized water until the liquid above became colorless, and dried at 60 degrees Celsius for a period of 24 hours (Scheme 1).

2.4 Instrumentation and characterization

The following analytical techniques were used to investigate the physicochemical properties, morphological features, and sensing performance of the synthesized materials. Powder X-ray diffraction patterns were recorded on a Siemens diffractometer

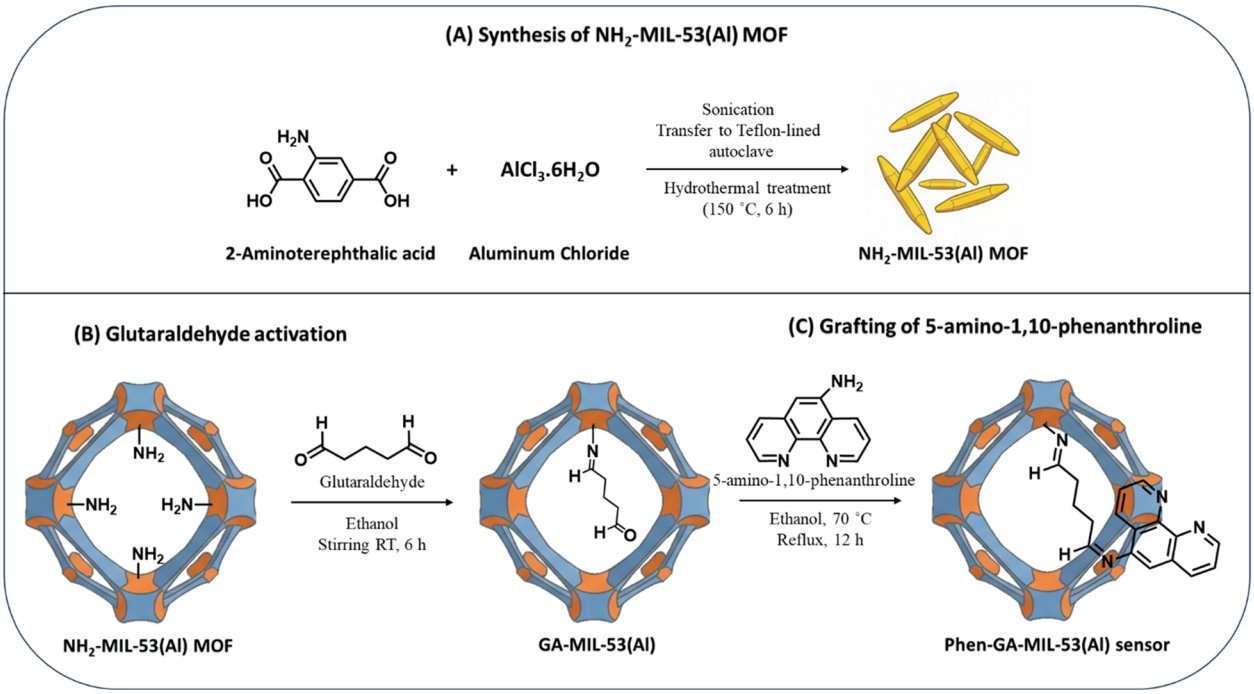

Scheme 1 Illustration of the synthesis of NH_2-MIL-53(Al), and Phen-GA-MIL-53(Al) sensor.

model D500 from Germany with Cu–K radiation source (wavelength 1.54 Angstroms) operating at 30 kV and 20 mA. The surface microstructure was visualized using Scanning Electron Microscopy which is JSM-6510LV from JEOL Ltd Tokyo Japan. Elemental mapping and semi-quantitative analysis were done through Energy Dispersive X-ray Spectroscopy at an accelerating voltage between 15 to 20 kV. Fourier Transform Infrared spectra were obtained with A Nicolet IS10 Fourier transform infrared spectrometer covering the range of 4000–400 cm^{-1} by the KBr pellet method. Overlapping peaks and sequential interactions were resolved by processing two-dimensional correlation spectroscopy with Origin lab. Nitrogen adsorption–desorption isotherms were measured at 77 K using Quantachrome Instruments Anton Paar Quanta Tec Inc surface area and porosity analyzer. The specific surface area was determined by the Brunauer–Emmett–Teller method while pore size distribution was computed *via* Barrett–Joyner–Halenda model. All UV-Vis absorption spectra as well as "naked-eye" colorimetric data were taken on a HACH DR 5000 UV VIS Spectrophotometer in a quartz cuvette of path length 1 cm. For real sample validation, As^{3+} and Fe^{2+} concentrations were cross-verified using Inductively Coupled Plasma Optical Emission Spectroscopy Varian 710-ES.

2.5 Computational details

The theoretical modeling and density functional theory (DFT) calculations for the designed sensing unit (2) consisting of a specific ligand and metal coordination was carried out using the Gaussian 09w software. The truncated cluster model representing the Phen-GA-MIL-53(Al) sensing unit was obtained to execute the quantum chemical calculations. Therefore, in the truncated cluster model, on one side the 5-amino-1,10-phenanthroline ligand is bound to glutaraldehyde spacer and on the other side a 2-aminoterephthalate linker is also attached to the Al(III) center (4). The simulation studies and calculations carried out in this research are based on the B3LYP level of theory combined with the 6-31G(d) basis set which allows an accurate description of the electonic properties of the molecular systems under study (5). For the computation of the effective core potential for the Al(II) metal center, LANL2DZ was employed (6). To verify the correctness of the extracted optimized molecular structure, frequency calculations were performed. To inspect the structural integrity of the target configuration, frequency calculations were also performed with the optimized models (7). The calculations were carried out with the computed model in the gas phase to clearly observe electronic redistribution on excited state events (8). The resulting values of the HOMO–LUMO energy gaps in the excited state showed shifts in the spectrum. The shift of the HOMO and LUMO electrons was detected simultaneously with the shift of the energies of these molecular orbitals (9). The computational process were carried out in the GaussView 6.0 package (10).

2.6 General procedure for spectrophotometric detection

Spectrophotometric titrations were used to study the sensing properties of the Phen-GA-MIL-53(Al) Sensor towards As^{3+} and Fe^{2+} ions in solution. In each experiment, 0.5 mg of the Phen-GA-MIL-53(Al) Sensor was dispersed into 20 mL of deionized water by gentle ultrasonication. Different amounts of As^{3+} and Fe^{2+} ions were then added. During the UV–Vis spectrophotometry study, absorbance spectra were recorded from 200 to 600 nm with special attention to changes in metal-to-ligand

charge transfer (MLCT). The selectivity test involved common competing metal ions (Na^+, K^+, Ca^{2+}, Mg^{2+}, Cu^{2+}, Ni^{2+}, Pb^{2+}, Co^{2+}, Zn^{2+}, Hg^{2+}, Cl^-, NO_3^-, SO_4^{2-} and PO_4^{3-}) under similar experimental conditions. The sensor gave a strong optical response only with As^{3+} and Fe^{2+} indicating high selectivity. Studies on pH stability found that the best sensing ranges for As^{3+} at pH 4.0 and for Fe^{2+} at pH 7.0. Also, regeneration of the sensor was achieved by washing with Thiourea and EDTA followed by ethanol for As^{3+} and Fe^{2+} respectively; performance was continuously kept up over six consecutive cycles.

2.7 Analytical applications in real samples

To evaluate the real-world effectiveness of the Phen-GA-MIL-53(Al) Sensor in complex mixtures, tests were carried out on actual environmental water samples. Local tap water samples were collected and then filtered through membranes with a pore size of 0.45 μm. Dilute HNO_3 was used to adjust the pH of the samples down to pH 2.0. Standard additions of As^{3+} and Fe^{2+} at concentrations of 50, 100, and 200 ppb were spiked into 20 mL portions of each sample. The same method was applied for determining Fe^{2+} ions in a pharmaceutical sample (dietary supplement). After removing the caps, ten Feroglobin capsules were poured into 50 mL of 50% HNO_3 (v/v). The solution was heated until nearly dry and then transferred to a volumetric flask with a 100 mL mark. Immediately after preparing the solution to volume, one milliliter was serially diluted in different graduated 20 mL flasks using appropriate buffer solutions. An aliquot of Phen-GA-MIL-53(Al) Sensor, equal to 0.5 mg in 20 mL, was added and both UV–Vis absorbance data collected after equilibration time. Recoveries and relative standard deviations (RSD) were used to check the accuracy and precision of the analysis.

3. Result and discussion

3.1 Structural and morphological characterization

3.1.1 Phase purity and crystallinity (XRD). The X-ray diffraction (XRD) pattern of the synthesized Phen-GA-MIL-53(Al) sensor Fig. 1A displays a series of sharp and well-resolved diffraction peaks within the 2θ range of 10–30°, confirming the highly crystalline nature of the material and the successful formation of the MIL-53(Al) framework. The prominent reflections observed at approximately $2\theta \approx 12.5°$, 17.8°, 20.3°, 25.6°, and 27.4° are consistent with the characteristic crystallographic planes of NH_2-MIL-53(Al), indicating that the periodic porous structure of the parent MOF was preserved after post-synthetic functionalization.[27] Notably, after the incorporation of 5-amino-1,10-phenanthroline molecules, no additional diffraction peaks related to free phenanthroline were detected; however, a slight decrease in peak intensity along with minor peak broadening was observed, which can be attributed to the successful immobilization of phenanthroline moieties onto the internal surface of the MOF channels through coordination interactions and/or glutaraldehyde-mediated Schiff base linkage.[28] The retention of the main diffraction peaks without the appearance of impurity phases demonstrates that the functionalization process occurred without structural collapse or distortion of the NH_2-MIL-53(Al) framework, thereby confirming that the crystalline architecture and long-range order of the MOF were maintained, which is essential for preserving the accessible active sites required for the selective sensing performance toward As^{3+} and Fe^{2+} ions as discussed in the manuscript Fig. 1A.

3.1.2 BET surface area. The N_2 adsorption–desorption isotherms of NH_2-MIL-53(Al) and Phen-GA-MIL-53(Al) sensor, measured at 77 K Fig. 1B, exhibit a typical type IV isotherm with a pronounced H_3-type hysteresis loop in the relative pressure (P/P_0) range of 0.4–1.0, indicating the presence of mesoporous structures with slit-shaped pores arising from the aggregation of MOF crystallites. The pristine NH_2-MIL-53(Al) sample demonstrates a high BET surface area of 1708.6 $m^2\ g^{-1}$, a pore radius of 1.84 nm, and a total pore volume of 1.82 $cm^3\ g^{-1}$, confirming its well-developed porous framework and large accessible surface area.[29] Upon functionalization with 5-amino-1,10-phenanthroline to form Phen-GA-MIL-53(Al) sensor, a noticeable decrease in nitrogen uptake is observed across the entire P/P_0 range, accompanied by a reduction in BET surface area to 1384 $m^2\ g^{-1}$, pore radius to 1.62 nm, and total pore volume to 1.32 $cm^3\ g^{-1}$. This decline in textural parameters can be attributed to the successful immobilization of phenanthroline molecules within the internal pores and onto the surface of the NH_2-MIL-53(Al) framework, leading to partial pore filling and blockage, which consequently limits the accessibility of nitrogen molecules to the adsorption sites without causing any collapse of the MOF structure Fig. 1B.

3.1.3 FTIR analysis. The FT-IR spectra of Phen-GA-MIL-53(Al) sensor and Fe^{2+}@Phen-GA-MIL-53(Al), shown in, were recorded in the range of 4000–500 cm^{-1} to investigate the functional groups involved Fig. 1C in the sensing process and to confirm the interaction between Fe^{2+} ions and the modified MOF framework. For Phen-GA-MIL-53(Al) sensor, the broad absorption band observed around 3400–3300 cm^{-1} is attributed to the stretching vibration of $-NH_2$ groups, while the bands located at approximately 1650–1570 cm^{-1} correspond to the C=O stretching and aromatic C=C vibrations of the organic linker.[30] The characteristic peaks in the region of 1400–1250 cm^{-1} are assigned to C–N stretching vibrations associated with the incorporated phenanthroline ligand. Additionally, the bands appearing at around 750–600 cm^{-1} are related to Al–O vibrations of the metal–organic framework skeleton. After adsorption of Fe^{2+} ions, noticeable shifts in the positions and intensities of these characteristic bands were observed, particularly in the C=N and C–N stretching regions, indicating the involvement of nitrogen donor atoms in coordination interactions with Fe^{2+} ions. Furthermore, slight changes in the Al–O vibration bands suggest the participation of oxygen-containing functional groups in the binding process.[31] These spectral modifications confirm the successful complexation of Fe^{2+} ions with the phenanthroline-functionalized NH_2-MIL-53(Al), thereby validating the sensing mechanism based on metal–ligand coordination interactions Fig. 1C.

The synchronous and asynchronous two-dimensional correlation spectroscopy (2D-COS) FT-IR spectra of the Phen-

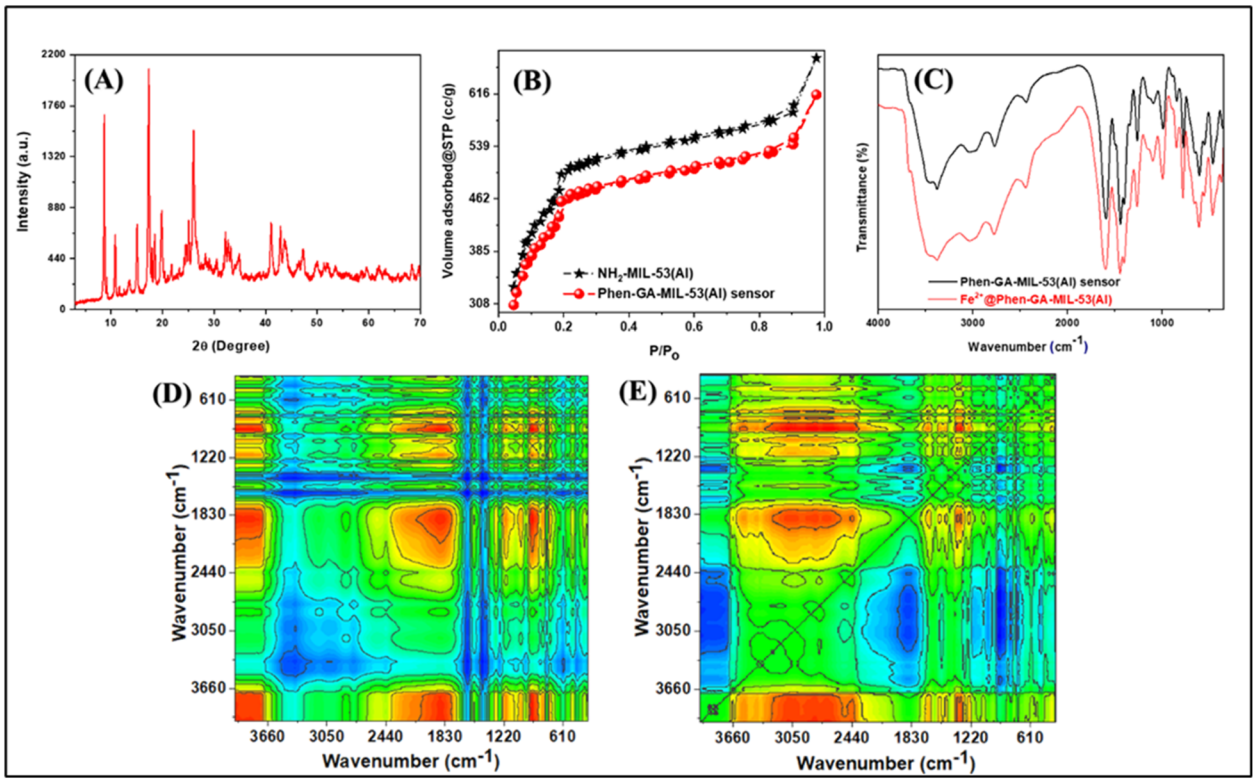

Fig. 1 (A) XRD pattern of Phen-GA-MIL-53(Al) sensor, (B) N_2 adsorption/desorption isotherm of NH_2-MIL-53(Al) MOF and Phen-GA-MIL-53(Al) sensor, (C) FT-IR of Phen-GA-MIL-53(Al) sensor, and Fe^{2+}@Phen-GA-MIL-53(Al) sensor, (D) synchronous, and (E) asynchronous between Phen-GA-MIL-53(Al) sensor, and Fe^{2+}@Phen-GA-MIL-53(Al) sensor.

GA-MIL-53(Al) sensor before and after interaction with metal ions are presented in Fig. 1D and E, respectively, to provide deeper insight into the sequence of functional group interactions during the sensing process.[32] The synchronous spectrum Fig. 1D exhibits several auto-peaks along the diagonal region, particularly in the ranges of 3600–3000 cm^{-1}, 1800–1500 cm^{-1}, and 1200–600 cm^{-1}, which are attributed to $-NH_2$ stretching vibrations, C=N/C–N functional groups of the phenanthroline ligand, and Al–O framework vibrations, respectively. The presence of strong cross-peaks between these regions indicates simultaneous variations in the vibrational intensities of nitrogen- and oxygen-containing functional groups upon coordination with metal ions. In contrast, the asynchronous spectrum Fig. 1E reveals off-diagonal cross-peaks that provide information about the sequential order of spectral intensity changes, suggesting that the coordination process initially involves the nitrogen donor atoms of the phenanthroline ligand followed by the participation of oxygen-containing groups within the MOF framework. These findings confirm that the sensing mechanism is governed by a synergistic coordination interaction between the metal ions and the active N- and O-binding sites of Phen-GA-MIL-53(Al) sensor, thereby validating the effective role of the functionalized MOF structure in selective metal ion recognition.[33]

3.1.4 EDX analysis. The elemental composition of the synthesized Phen-GA-MIL-53(Al) sensor was investigated using energy-dispersive X-ray (EDX) spectroscopy, as illustrated in Fig. 2A. The EDX spectrum confirms the presence of the main constituent elements, including carbon (C), nitrogen (N), oxygen (O), and aluminum (Al), which are integral components of both the NH_2-MIL-53(Al) framework and the incorporated 5-amino-1,10-phenanthroline ligand. Quantitative analysis revealed that the elemental weight percentages of C, N, O, and Al were 13.86%, 15.11%, 24.46%, and 46.57%, respectively. The relatively high aluminum content verifies the formation of the Al-based metal–organic framework, while the presence of nitrogen is attributed to both the amino functional groups of the terephthalic linker and the nitrogen-rich phenanthroline molecules successfully immobilized onto the MOF structure.[34] The absence of any additional impurity-related elemental peaks in the spectrum further indicates the high purity of the synthesized material and confirms that the functionalization process did not introduce any undesirable contaminants, thereby supporting the successful preparation of the Phen-GA-MIL-53(Al) sensor sensing platform Fig. 2A.

The successful adsorption of As^{3+} ions onto the Phen-GA-MIL-53(Al) sensor was further confirmed by energy-dispersive X-ray (EDX) analysis, as shown in Fig. 2B. The EDX spectrum of As^{3+}@Phen-GA-MIL-53(Al) reveals the presence of characteristic peaks corresponding to carbon (C), nitrogen (N), oxygen (O), aluminum (Al), and a newly emerged peak assigned to arsenic (As), indicating the effective binding of As^{3+} ions onto the functionalized MOF surface.[35] The quantitative elemental analysis demonstrated that the weight percentages of C, N, O,

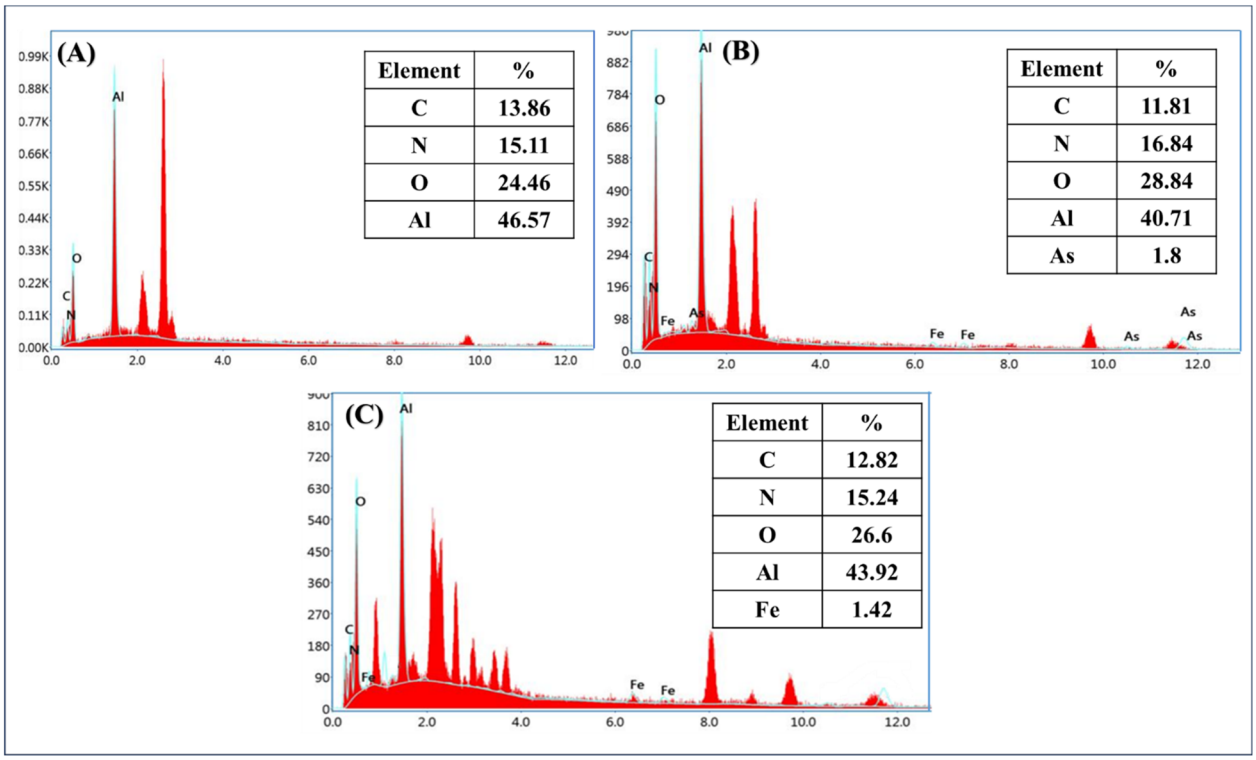

Fig. 2 (A) EDX analysis of Phen-GA-MIL-53(Al) sensor, (B) As^{3+}@Phen-GA-MIL-53(Al) complex, and (C) Fe^{2+}@Phen-GA-MIL-53(Al) complex.

Al, and As were 11.81%, 16.84%, 28.84%, 40.71%, and 1.8%, respectively. The appearance of the arsenic signal, which was absent prior to metal ion exposure, clearly confirms the successful uptake of As^{3+} ions by the phenanthroline-modified NH_2-MIL-53(Al) framework. Moreover, the slight reduction in aluminum content after adsorption suggests the involvement of coordination interactions between As^{3+} ions and the nitrogen-containing phenanthroline ligand as well as oxygen functional groups present in the MOF structure, thereby validating the formation of stable surface complexes responsible for the sensing and adsorption performance of the developed material Fig. 2B.

The adsorption of Fe^{2+} ions onto the Phen-GA-MIL-53(Al) sensor was confirmed by energy-dispersive X-ray (EDX) analysis, as depicted in Fig. 2C. The obtained EDX spectrum demonstrates the presence of the primary framework elements, namely carbon (C), nitrogen (N), oxygen (O), and aluminum (Al), along with the apperence of new characteristic peaks corresponding to iron (Fe), which verifies the successful interaction and immobilization of Fe^{2+} ions onto the functionalized MOF surface.[36] The quantitative elemental composition revealed that the weight percentages of C, N, O, Al, and Fe were 12.82%, 15.24%, 26.6%, 43.92%, and 1.42%, respectively. Notably, the appearance of the Fe signal, which was absent in the pristine Phen-GA-MIL-53(Al) sensor, clearly indicates the effective uptake of Fe^{2+} ions through coordination interactions with the nitrogen donor atoms of the phenanthroline ligand and oxygen-containing functional groups of the MOF framework. Furthermore, the slight variation in the elemental distribution after adsorption suggests the formation of stable surface complexes between Fe^{2+} ions and the active binding sites of the sensor, thereby confirming the capability of the phenanthroline-functionalized NH_2-MIL-53(Al) for selective metal ion sensing applications Fig. 2C.

3.1.5 SEM mapping. The surface morphology and elemental distribution of the synthesized Phen-GA-MIL-53(Al) sensor were further examined by SEM coupled with elemental mapping analysis, as illustrated in Fig. 3A. The SEM image reveals that the material possesses a clustered and agglomerated morphology composed of irregularly shaped crystallites, which is typical for MIL-53(Al)-based frameworks.[37] The corresponding elemental mapping images confirm the homogeneous spatial distribution of carbon (C), nitrogen (N), oxygen (O), and aluminum (Al) throughout the entire surface of the material without any noticeable phase segregation or elemental accumulation. The uniform dispersion of aluminum indicates the integrity of the MOF backbone, while the well-distributed nitrogen signal verifies the successful incorporation of nitrogen-rich phenanthroline molecules within the NH_2-MIL-53(Al) framework. Quantitative analysis shows that the elemental composition consists of 12.6% C, 14.2% N, 21% O, and 52.2% Al, which is consistent with the expected chemical structure of the functionalized MOF. This uniform elemental distribution suggests that the post-synthetic modification with phenanthroline occurred effectively over the MOF surface and internal pores without disrupting the structural framework, thereby supporting the formation of a stable sensing platform.

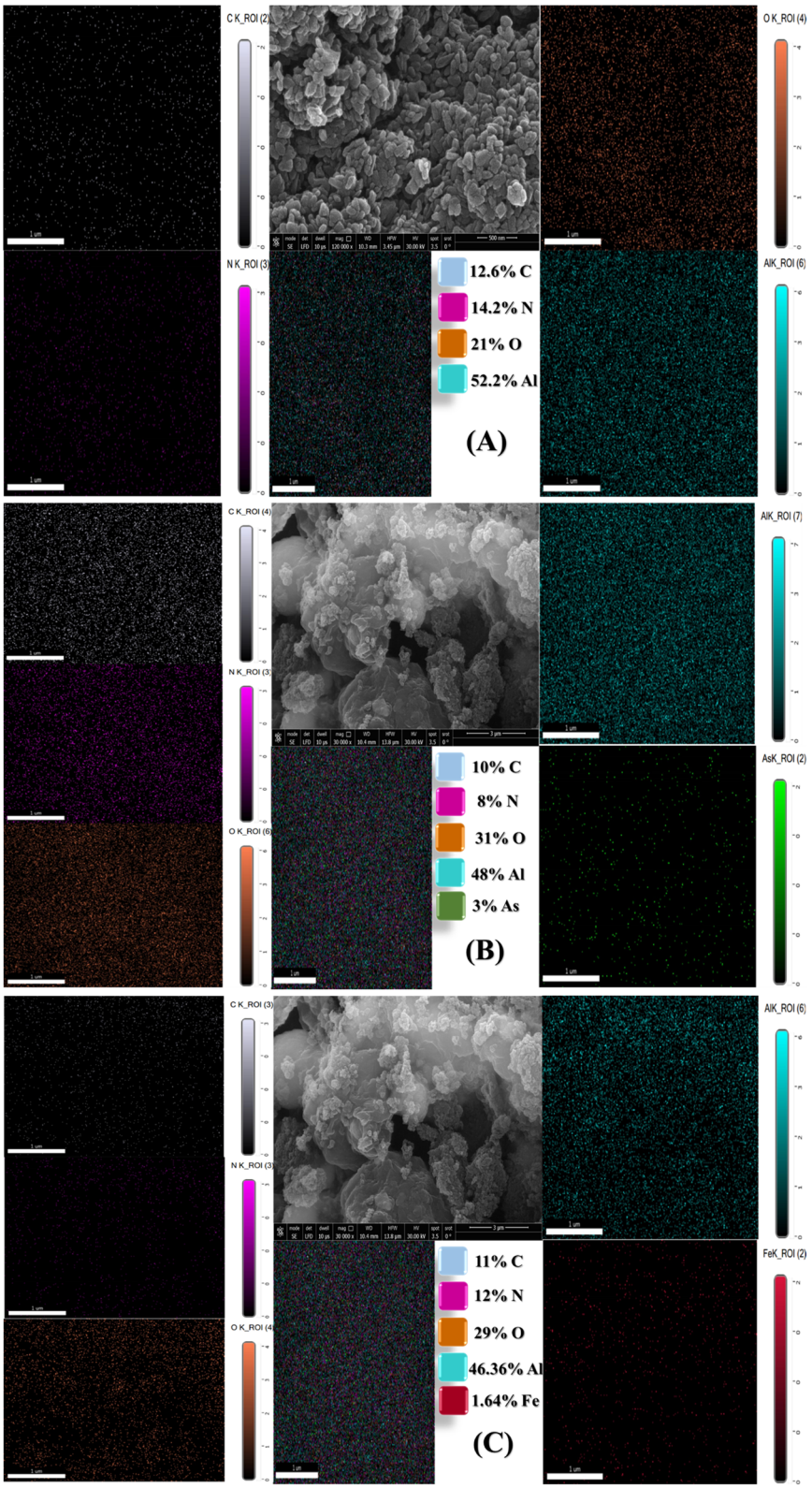

Fig. 3 (A) SEM mapping analysis of Phen-GA-MIL-53(Al) sensor, (B) As^{3+}@Phen-GA-MIL-53(Al) complex, and (C) Fe^{2+}@Phen-GA-MIL-53(Al) complex.

The SEM–EDX elemental mapping analysis of As^{3+}@Phen-GA-MIL-53(Al), as presented in Fig. 3B, was carried out to investigate the surface morphology and confirm the successful adsorption of As^{3+} ions onto the functionalized MOF framework. The SEM micrograph reveals that the material maintains its aggregated and clustered morphology after metal ion uptake,

indicating that the adsorption process did not cause any structural deformation or collapse of the phenanthroline-modified NH_2-MIL-53(Al). The corresponding elemental mapping images demonstrate a uniform distribution of carbon (C), nitrogen (N), oxygen (O), and aluminum (Al) across the surface, along with the apperance of a distinct arsenic (As) signal homogeneously dispersed throughout the material.[38] Quantitative mapping analysis indicates elemental compositions of approximately 10% C, 8% N, 31% O, 48% Al, and 3% As, confirming the successful immobilization of As^{3+} ions within the internal pores and on the external surface of the MOF. The homogeneous distribution of arsenic without localized aggregation suggests that the adsorption occurred *via* coordination interactions between As^{3+} ions and the nitrogen- and oxygen-containing functional groups of the Phen-GA-MIL-53(Al) sensor, thereby validating its effectiveness for arsenic sensing applications.

The SEM–EDX elemental mapping analysis of Fe^{2+}@Phen-GA-MIL-53(Al), as illustrated in Fig. 3C, was conducted to evaluate the morphological stability and confirm the successful adsorption of Fe^{2+} ions onto the functionalized MOF framework. The SEM image shows that the material preserves its aggregated and clustered surface morphology after Fe^{2+} uptake, indicating that the adsorption process did not induce any noticeable structural collapse of the phenanthroline-modified NH_2-MIL-53(Al). The corresponding elemental mapping images reveal a homogeneous spatial distribution of carbon (C), nitrogen (N), oxygen (O), and aluminum (Al), along with the emergence of a distinct iron (Fe) signal uniformly dispersed throughout the material surface. Quantitative analysis indicates elemental compositions of approximately 11% C, 12% N, 29% O, 46.36% Al, and 1.64% Fe, confirming the effective immobilization of Fe^{2+} ions within the MOF pores and on the external surface. The uniform dispersion of iron without localized clustering suggests that Fe^{2+} adsorption occurred through coordination interactions with the nitrogen donor atoms of the phenanthroline ligand and oxygen-containing functional groups of the NH_2-MIL-53(Al) framework, thereby validating the sensing capability of the developed material toward Fe^{2+} ions.[39]

3.2 Optimization of sensing conditions

3.2.1 Effect of pH. The pH value of the water solution is an important factor that affects how sensitive the Phen-GA-MIL-53(Al) sensor is. This is because it changes the protonation state of the nitrogen donors in phenanthroline and the chemical form of the target ions.[40] The sensing ability was tested from a pH of 2.0 to 10.0 to find where the spectrophotometric response was highest, as shown in Fig. 4A.

The max absorbance for As^{3+} was at pH 4.0. It is under acidic pH that the surface of the sensor Phen-GA-MIL-53(Al) has a certain charge distribution to favor interaction with the arsenite species. Even though $As3^{+}$ mainly exists in neutral form as H_3AsO_3 at this pH ($pK_{a1} = 9.2$), high sensitivity in acidic media may be due to best orientation of anchored phenanthroline-glutaraldehyde moieties which help interaction between arsenic center and modified pore environment. Signal decrease below pH 3.0 probably results from over-protonation of functional sites on the framework leading to either structural transition or electrostatic repulsion.

For Fe^{2+}, the optimal sensing response occurred at pH 7.0, accompanied by a vivid and instantaneous color transition from colorless to orange. This chromogenic change is characteristic of the formation of the tris-complex $[Fe(phen)_3]^{2+}$ within the MOF scaffold. At pH 7.0, the nitrogen atoms of the phenanthroline ligand are fully deprotonated ($pK_a = 4.9$), providing an electron-rich environment ideal for coordinating the Fe^{2+} center. At lower pH values (pH < 5.0), the absorbance intensity dropped significantly because the competition between H^+ ions and Fe^{2+} for the nitrogen lone pairs inhibits complexation. Conversely, beyond pH 8.0, the signal declined as a result of the onset of Fe^{2+} hydrolysis and the formation of iron hydroxides.

3.2.2 Effect of sensor dosage. The effect of the amount of Phen-GA-MIL-53(Al) on As^{3+} and Fe^{2+} detection was studied by changing adsorbent mass from 2 to 8 mg in a constant analyte solution volume of 20 mL at their respective optimal pH values, as shown in Fig. 4B.

For both ions, the absorbance intensity increased progressively with an increase in the sensor dosage from 2 mg to 6 mg.[41] This phenomenon can be directly attributed to the increased surface area and higher density of phenanthroline-glutaraldehyde moieties anchored for interaction. More active sites exposed mean that a greater percentage of As^{3+} and Fe^{2+} ions are captured from the aqueous phase, resulting in a more intense colorimetric signal.

After 6 mg, there was no further increase in the absorbance signal. This is known as saturation and happens when the concentration of the target analytes becomes limiting; when almost all ions in solution are chelated by excess sensor material, increasing the dose further does not produce any more spectrophotometric change. Also, in solid-state sensing too much material can result in "optical crowding" or light scattering which could reduce the signal-to-noise ratio slightly. According to these results, 6 mg was chosen as the standard amount for future experiments. This mass offers the best compromise between high sensitivity and analytical economy, thus maintaining a highly efficient sensor for trace-level detection.

3.2.3 Effect of contact time. The evaluation of kinetics must be thoroughly evaluated for their suitability in the design of solid-state sensors for applications in various fields such as environmental monitoring. These sensors are advantageous as they allow for the real-time monitoring of dangerous pollutants, leading to rapid response decreases in contamination levels. The absorbance of Phen-GA-MIL-53(Al) was recorded at the intervals from 0 to 80 s after exposure to As^{3+} and Fe^{2+} ions to find out the least time needed for attaining a stable spectrophotometric signal. Analytes were very fast interacting with the functionalized framework, as shown in Fig. 4C. The As^{3+} ions showed fast binding kinetics, reaching a stable plateau in 50 s. This is slightly slower than the transition metal coordination of Fe^{2+}, but still highly competitive for solid-state sensors. The interaction is based on hydrogen bonding and Lewis acid-base recognition, and benefits from the high density of imine and

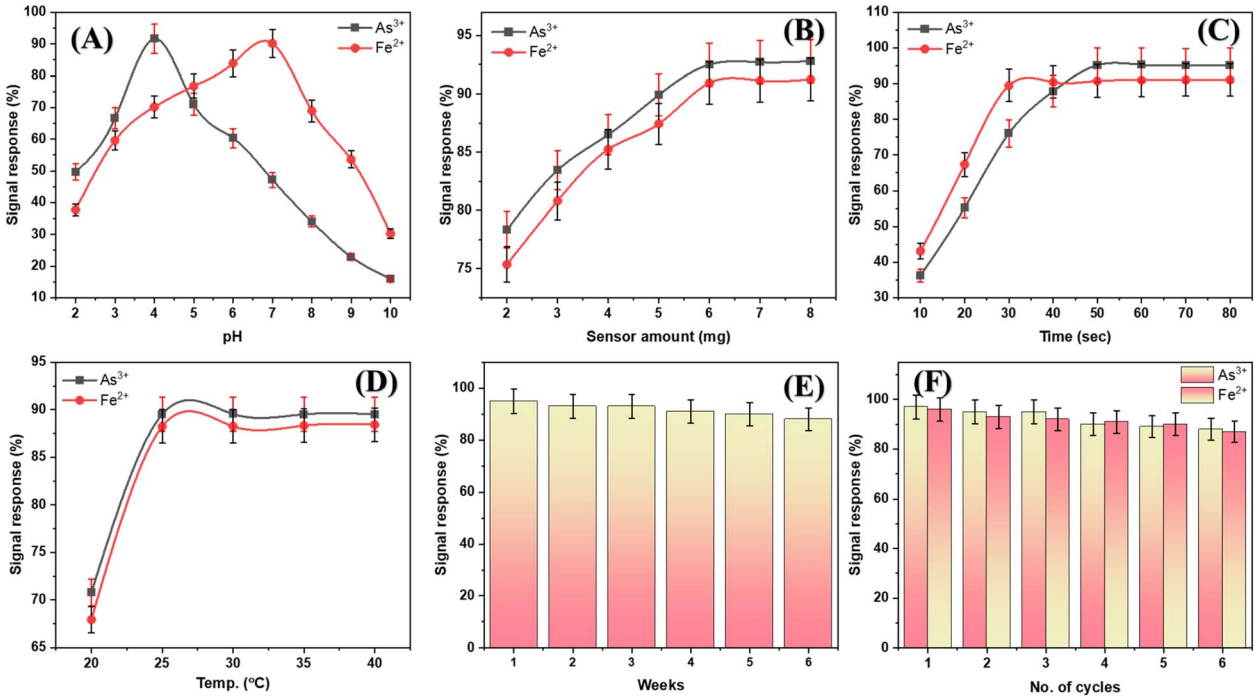

Fig. 4 Analytical parameters assessment for the recognition of As^{3+} and Fe^{2+} ions with the Phen-GA-MIL-53(Al) sensor, in terms of signal response (%) as a function of pH solution (A), Phen-GA-MIL-53(Al) sensor amount (B), reaction time (C) reaction temperature (D), stability studies (E) and reusability (F). Error bars represent the standard deviation of triplicate measurements ($n = 3$).

phenanthroline nitrogen sites that are anchored within the MOF pores. The response for Fe^{2+} also was practically immediate. A change in color to orange-red was seen within seconds of contact, and the absorbance signal achieved its maximum value in 30 seconds. Such quick performance can be attributed to the fact that the bidentate phenanthroline sites have a high affinity for Fe^{2+}, allowing them to form a stable complex of $[Fe(phen)_3]^{2+}$ with very little activation energy. The imprinted kinetic performance in Fig. 4C can be attributed to the structural merits of the NH_2-MIL-53(Al) template. Hierarchical porosity with a large internal surface area fosters rapid mass transport and minimizes intra-particle diffusion resistance. Moreover, the glutaraldehyde (GA) imprint efficiently projects the phenanthroline ligands into the pore voids, making them sterically accessible for aqueous ions.

3.2.4 Effect of temperature. The effect of temperature on the absorbance intensity of the Phen-GA-MIL-53(Al) conjugate material was studied systematically to find out the best thermal conditions for accurate detection and how stable the ligand–analyte complexes are. The experimental results in Fig. 3D show that the absorbance intensity for As^{3+} and Fe^{2+} remain nearly constant between 25 °C and 40 °C. The interaction between As^{3+}, governed by hydrogen bonding and Lewis acid-base sites, also does not significantly degrade within this ambient range. In the case of Fe^{2+}, its coordination with the 1,10-phenanthroline moiety to form the complex $[Fe(phen)_3]^{2+}$ is thermodynamically favorable and has high stability constants, meaning that the chromogenic response cannot easily be perturbed by moderate thermal energy.

3.2.5 Storage stability and shelf-life assessment. The long-term stability and sensing performance of phen-GA-MIL-53(Al) were examined in detail for its further application in environmental monitoring. To test the stability of phen-GA-MIL-53(Al), the adsorbent was kept at 25 °C in desiccator for 6 weeks. The absorbance spectra were obtained from the second day to the 42 day (*i.e.*, the second day, 4 day, 7 day, 14 day, 21 day, 28 day, 35 day, and 42 day), and the absorbance intensity of As^{3+} and Fe^{2+} was retained for 95% of its initial value (Fig. 5A), suggesting that the phen-GA-MIL-53(Al) have an excellent stability. Further, the stability of the sensor was confirmed to be better than those of our previous studies or the existing literature (Table S1). Those superior sensing properties could be attributed to covalent bonds formation between the NH2-MIL-53(Al) framework and glutaraldehyde and 5-amino-1,10-phenanthroline (*i.e.*, the phen-GA-MIL-53(Al)), as well as the hydrolytic stability of the Al-carboxylate framework of the parent NH2-MIL-53(Al) 15 (as shown in the stability section). The positively charged Al^{3+} in MIL-53 framework can propagate the wealth of charge by forming charge-dense clusters and reducing the electrostatic charge of the Al^{3+} ions. In addition, MIL-53 also exhibits a special 'gate-opening' mechanism, which indicates that the framework is stable in the unfilled state and is able to undergo large structural change upon guest adsorption. Therefore, the great stability of the sensor is attributed to the rigidity of the MOF structure.

3.2.6 Reusability studies. The reusability of the Phen-GA-MIL-53(Al) sensor was evaluated for its economic and ecological performance, being one of the critical characteristics for

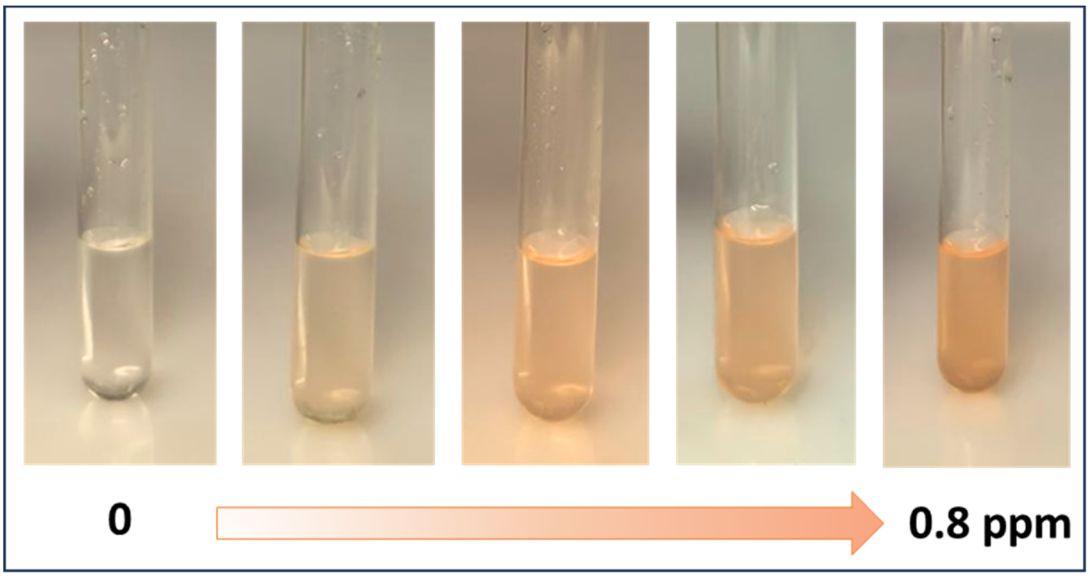

Fig. 5 Colorimetric response of the Phen-GA-MIL-53(Al) sensor showing gradual fading from colorless to light orange with increasing Fe^{2+} ions concentration.

MOF materials. The sensor was regenerated with 0.1 M Thiourea for As^{3+}, and thereafter with 0.1 M EDTA for Fe^{2+}. The regenerated Phen-GA-MIL-53(Al) sensor after each cycle was tested with As^{3+} or Fe^{2+} ions. As observed in Fig. 6a and b, the working curves of the regenerated Phen-GA-MIL-53(Al) sensor overlap with the original working curves and exhibit similar fluorescence intensity and quenching degree. The signal-tonoise ratio of the Phen-GA-MIL-53(Al) sensor maintains at the same level after six regeneration cycles, indicating the high efficiency of the regeneration step (Fig. 6c). The minor performance decline is likely due to mechanical loss during the regeneration step, implying that the Phen-GA-MIL-53(Al) sensor has unlimited reusability. As observed in X-ray diffraction (XRD) patterns (Fig. 6d), the XRD pattern of the six-time regenerated

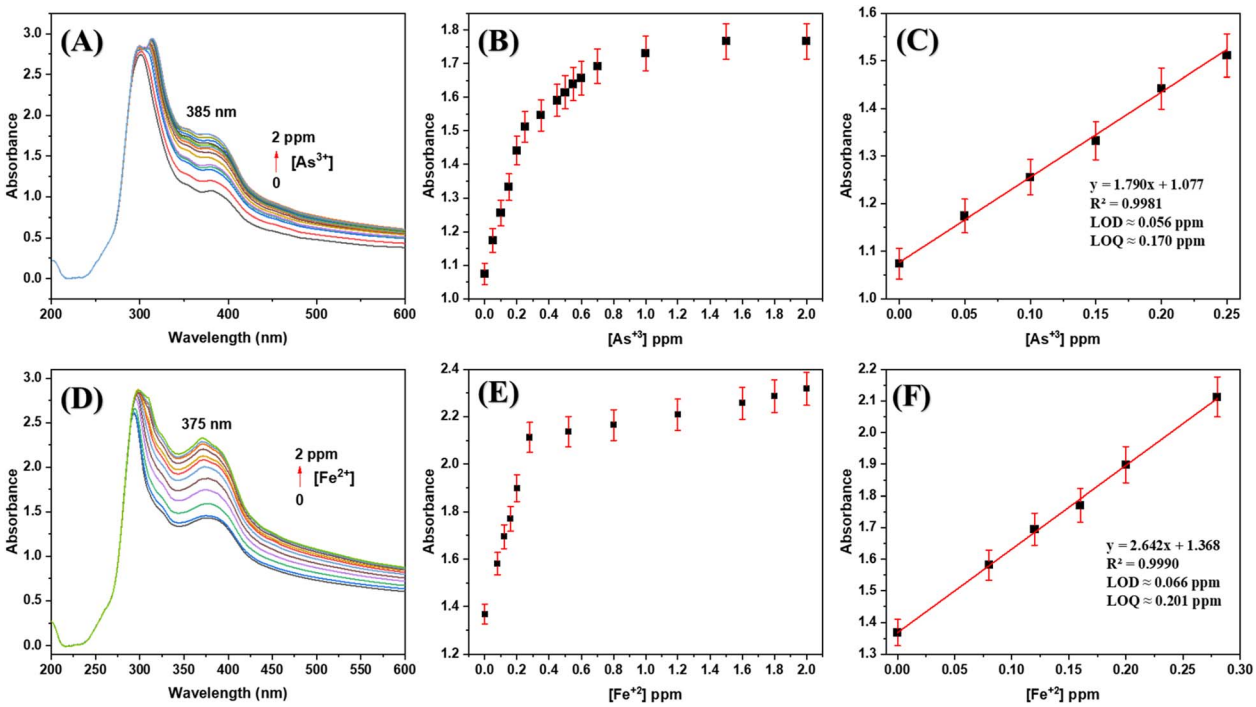

Fig. 6 Quantitative spectrophotometric sensing performance of Phen-GA-MIL-53(Al): (A, D) absorption spectra as a function of increasing analyte concentration; (B, E) non-linear concentration profiles; and (C, F) linear calibration curves for As^{3+} (pH 4.0) and Fe^{2+} (pH 7.0). Data points represent the mean of three independent trials ($n = 3$), with error bars indicating the standard deviation (±SD).

Phen-GA-MIL-53(Al) is almost the same as that of the original Phen-GA-MIL-53(Al) material, confirming the stability of the material. The covalent design of the Phen-GA-MIL-53(Al) sensor also prevents ligand leaching during the continuous regeneration of the sensor. The regeneration step of the Phen-GA-MIL-53(Al) obeys the following reaction mechanism: the chelation of thiourea or EDTA with As^{3+} and Fe^{2+} ions results in the release of the ligand from the Phen-GA-MIL-53(Al) sensor, while reducing As^{3+} and Fe^{2+}, respectively. Regeneration was carried out without losing the Phen-GA-MIL-53(Al) material *via* the developed method, making it possible to carry out the regeneration step multiple times, which provides a clear environmental advantage over organic materials that cannot be regenerated. Moreover, regeneration contributes to making the MOF materials available for multiple analysis, which also provides an economic advantage. Such a high performance with reusability of the Phen-GA-MIL-53(Al) sensor indicates that it is an ideal sensing material for practical applications.

3.3 Detection performance

3.3.1 Naked-eye responses. The practical use of the Phen-GA-MIL-53(Al) sensor was first tested by looking at its color change with the naked eye. This gave a quick and qualitative "on-off" signal for detecting Fe^{2+}. As seen in Fig. 5, the functionalized metal–organic framework scaffold works as a very sensitive chromoionophoric probe. It shows a bright and orderly color change when it comes into contact with higher amounts of Fe^{2+} ions at pH 7.0. The first color of the Phen-GA-MIL-53(Al) sensor is a colorless. When Fe^{2+} is added, the material visibly changes to a light orange color at very low amounts. Increasing the amount of Fe^{2+} from 0 to 2 ppm results.

This large change in color is a clear sign of the tris-complex $[Fe(phen)_3]^{2+}$ forming inside the big pores of Al-MOF. The strong orange color comes from the transitions of Metal-to-Ligand Charge Transfer (MLCT) between the Fe^{2+} center and the 5-amino-1,10-phenanthroline parts that are stuck on through glutaraldehyde (GA) spacers. The high clarity of this color gradient makes it clear that GA linkers give enough room for these ligands to wrap effectively around iron ions even in such a close space as inside the framework.

3.3.2 Spectrophotometric detection of As^{3+} and Fe^{2+}. In order to give a rigorous quantitative basis for the observed naked-eye chromogenic changes, the spectrophotometric response of Phen-GA-MIL-53(Al) was taken as a function of analyte concentration. This analysis allows determination of the dynamic linear range and exact limits of detection for As^{3+} and Fe^{2+}.

The sensing performance for As^{3+} was tested at its best pH 4.0. When exposed to As^{3+}, a clear change in the absorption profile at 385 nm occurred, as seen in Fig. 6A. Unlike iron's coordination-driven MLCT, the response to As^{3+} is controlled by the interaction between arsenous acid species and imine/phenanthroline nitrogen sites through hydrogen bonding and Lewis acid-base recognition. This sensor has a broad linear response for As^{3+} from 0–2 ppm with a calculated limit of detection of 0.056 ppm.

The sensor Phen-GA-MIL-53(Al) shows absorption spectra after being exposed to different concentrations of Fe^{2+} 0–2 ppm at pH 7.0 in Fig. 6D. A strong absorption band appeared after the addition of Fe^{2+}, with a maximum wavelength at 375 nm. This peak is the known signature for the complex $[Fe(phen)_3]^{2+}$ and comes from metal-to-ligand charge transfer (MLCT) between an Fe^{2+} center and π^* orbitals on one of its ligands, which is 5-amino-1,10-phenanthroline. The intensity of this peak increased systematically with increasing iron concentration, mirroring the visual transition from colorless to orange.

3.3.3 Calibration curve and linearity. The quantitative ability of the sensor Phen-GA-MIL-53(Al) was systematically tested by establishing the relationship between the concentration of analyte and the resulting spectrophotometric response. Calibration curves were constructed under optimized conditions previously determined at pH 4.0 for As^{3+} and pH 7.0 for Fe^{2+}, with a fixed contact time and amount of sensor.

The detection of As^{3+} at pH 4.0 follows a linear response model, as illustrated in Fig. 6C. The sensor was linear over the entire range from 0 to 0.25 ppm. The regression equation also indicates that the hydrogen bonding and Lewis acid-base interaction of arsenous acid species with the functionalized framework is highly predictable and reproducible. Importantly, this sensor is still responsive at such low microgram levels, which would be important for monitoring arsenic in groundwater where concentrations are usually just below the regulatory threshold.

In Fig. 6F, the absorbance intensity at the characteristic wavelength of 375 nm showed a very strong linear increase with increasing concentrations of Fe^{2+}. The regression results indicated a linear equation for the concentration range from 0–0.28 ppm. The correlation coefficient R^2 was equal to 0.999, which means that it fitted excellently and can be used reliably for quantitative applications. This high value of slope (sensitivity) further indicates that $[Fe(phen)_3]^{2+}$ complex inside MOF pores has very strong molar absorptivity. Such high sensitivity is made possible by glutaraldehyde spacer because it ensures that phenanthroline moieties are extended enough into pore space to maximize coordination efficiency. Method sensitivity was expressed in terms of Limit of Detection (LOD) and Limit of Quantification (LOQ) calculated based on standard IUPAC definitions.

$$\mathrm{LOD} = 3\sigma/S \quad (1)$$

$$\mathrm{LOQ} = 10\sigma/S \quad (2)$$

Where σ is the standard deviation and S is the slope of the calibration curve. The computed LOD values were 0.056 ppm for As^{3+} for Fe^{2+} and 0.066 ppm for Fe^{2+}. These values are proving the potential of Phen-GA-MIL-53(Al) for ultra-trace environmental analysis. The construction of calibration curves for As^{3+} and Fe^{2+} ions required the aforementioned protocol on the optimized pH *i.e.* pH 4.0 for As^{3+} and pH 7.0 for Fe^{2+}. All the measured data were taken in triplicate ($n = 3$) to obtain the

mean value and their standard deviation for lesser error and hence higher precision. The optimized protocols have been then used to construct the calibration curves which gives the amount of As^{3+} and Fe^{2+} ions in the given water samples by comparing with the obtained standard curves. As the calibration curves for each of the ions are already established, a simple and quick method of exploring the capability of Phen-GA-MIL-53(Al) platform in As^{3+} and Fe^{2+} sensing is possibly through the comparison of standard curves for these two ions (Table 1). The developed platform is very sensitive and accurate in both the ion-sensing capabilities.[42,43]

A critical analysis of the analytical figures of merit summarized in Table 2 reveals that Phen-GA-MIL-53(Al) holds a distinct position among current state-of-the-art sensing platforms. While certain literature-reported sensors, such as BrPADAP for As^{3+} or Morin for Fe^{2+}, exhibit lower numerical LODs, they are frequently limited by narrow pH operating windows or susceptibility to signal quenching in real-world aqueous matrices. The Phen-GA-MIL-53(Al) sensor bridges this gap by offering high sensitivity well within the range required for environmental monitoring alongside exceptional structural robustness. The superiority of this platform is evidenced by three key factors, unlike the majority of reported sensors which are restricted to single-ion detection, our MOF-based system utilizes a pH-switchable mechanism to address two chemically distinct species (As^{3+} and Fe^{2+}) on a single material platform. The instantaneous naked-eye chromogenic response for Fe^{2+} provides a semi-quantitative tool for field screening that many high-precision electrochemical or ICP-based methods cannot replicate. The covalent anchoring of the phenanthroline-GA unit ensures that the sensor maintains ≈95% performance over six weeks and through six regeneration cycles, a significant improvement over physisorbed probes that often leach into the aqueous phase. Consequently, Phen-GA-MIL-53(Al) represents a strategically balanced sensing solution, trading extreme, lab-only sensitivity for the high-fidelity, dual-purpose performance required for practical environmental remediation.

3.4 Selectivity and interference performance

The practical effectiveness of any environmental sensor is determined by its capacity to selectively identify target substances in the midst of other ions that are present in a complex matrix. To assess how specific Phen-GA-MIL-53(Al) is, the response measured spectrophotometrically was tested against a number of potential interfering ions: Na^+, K^+, Ca^{2+}, Mg^{2+}, Cu^{2+}, Ni^{2+}, Pb^{2+}, Co^{2+}, Zn^{2+}, Hg^{2+}, Cl^-, NO_3^-, SO_4^{2-}, and PO_4^{3-}.

As shown in Fig. 7A and B, the Phen-GA-MIL-53(Al) sensor gave a very strong and different reaction only with As^{3+} at pH 4.0 and with Fe^{2+} at pH 7.0. The sensor kept a high response for As^{3+} because the special hydrogen-bonding network and Lewis acid-base sites inside the MOF pores very well "filter" the neutral arsenous acid from competing charged ions at the best acidic pH. To better simulate real-world conditions, interference studies were done by measuring how much the sensor reacts to target analytes in the presence of different concentrations of competing ions. Among the divalent transition metals that were present, only Fe^{2+} was able to trigger the typical orange chromogenic shift and the corresponding absorbance peak at 375 nm. This selectivity is attributed to the high stability constant of the $[Fe(phen)_3]^{2+}$ complex. The geometric arrangement of the phenanthroline ligands held by the glutaraldehyde spacer provides a "privileged" coordination environment for Fe^{2+}, perfectly suiting its ionic radius and electronic demands. To rigorously evaluate the diagnostic specificity of Phen-GA-MIL-53(Al), Fe^{3+} was included in the selectivity trials as a key redox-active competitor. As shown in the updated Fig. 7, the presence of Fe^{3+} did not result in significant signal interference for either analyte. For Fe^{2+} detection at pH 7.0, the high-spin Fe^{3+} state is effectively precluded from coordination due to the onset of hydrolysis and its inability to facilitate the specific MLCT transition required for the 375 nm absorbance peak. Similarly, the hydrogen-bonding pathway optimized for As^{3+}at pH 4.0 remains undisturbed by Fe^{3+}, as the framework's modified pore environment is specifically tuned to recognize non-dissociated arsenous acid. These findings underscore the sensor's capacity to discriminate between oxidation states, a critical requirement for accurate environmental monitoring.

As shown in Fig. 7A and B, the recovery of the As^{3+} and Fe^{2+} signals remained within the acceptable range of 95–105%. No significant signal suppression or enhancement was observed for most ions. Transition metals known to compete for nitrogen-donor ligands showed negligible interference due to "pore-size exclusion" and specific orientation of phenanthroline moieties favoring more stable iron complex formation and specific arsenic interaction. The elevated tolerance to typical groundwater components proves that Phen-GA-MIL-53(Al) is more than just a sensitive lab probe; it is a strong analytical platform appropriate for the direct examination of raw environmental water samples.

Table 1 Spectrophotometric parameters for Determination of the As^{3+} and Fe^{2+} Ions Using Phen-GA-MIL-53(Al) sensor

Parameter	As^{3+}	Fe^{2+}
pH	4.0	7.0
λ_{max} (nm)	385	375
Linear range	0.056–0.25	0.066–0.28
Correlation coefficient (R^2)	0.998	0.999
LOD (ppm)	0.056	0.066
LOQ (ppm)	0.170	0.201

3.5 Computational studies and theoretical validation

Density functional theory calculations were performed to clarify the electronic interactions and the nature of the chromogenic response of the Phen-GA-MIL-53(Al) sensor towards As^{3+} and Fe^{2+}. Structural optimizations and frontier molecular orbital analyses were carried out for this purpose. The Highest Occupied Molecular Orbital and the Lowest Unoccupied Molecular Orbital spatial distributions were used in these evaluations. The electronic properties of the functionalized sensing unit (Phenanthroline-GA moiety) were evaluated first.[52–54] As seen in

Table 2 Comparison of the analytical performance of Phen-GA-MIL-53(Al) sensor with other reported sensors

Target ion	Sensor material	Limit of detection (ppm)	Ref.
As^{3+}	BPBT	0.115	44
	BrPADAP	0.002	45
	Azure B	0.020	46
	Leuco malachite green	0.025	47
	Phen-GA-MIL-53(Al) sensor	0.056	This work
Fe^{2+}	Gold NR	0.0008	48
	2′,3,4′,5,7-Pentahydroxyflavone (morin)	0.0005	49
	2-(2-Pyridyl)imidazole (PIMH)	0.101	50
	CPR-H2O2	0.090	51
	Phen-GA-MIL-53(Al) sensor	0.066	This work

Fig. 8, the HOMO and LUMO for the free ligand are mainly distributed over the π-conjugated system of 5-amino-1,10-phenanthroline rings and imine (C═N) linkage. The computed energy gap for the uncomplexed sensor was – 0.1479. This rather large gap is in agreement with the fact that this material does not absorb in the visible range; hence it appears initially colorless.

The model used in computations for the interaction with As^{3+} shows a different electronic signature. The interaction of As^{3+} with the ligand includes hydrogen bonding and Lewis acid-base coordination between the arsenic center and nitrogen-rich imine/phenanthroline sites. FMO analysis indicates that there is an electron density redistribution upon arsenic binding, which makes the HOMO–LUMO gap decrease to −0.0646. Calculated stability confirms that Phen-GA-MIL-53(Al) has a very strong affinity for arsenite species in acidic media.

Coordination with Fe^{2+} causes an instant redistribution of the electronic density. The HOMO becomes largely confined to the d-orbitals of the Fe^{2+} site, while the LUMO stays primarily on the π* anti-bonding orbitals of the phenanthroline ligand. Such a situation presents a clear case for Metal-to-Ligand Charge Transfer (MLCT) since there is spatial separation between HOMO and LUMO. Coordination leads to substantial narrowing of the energy gap down to −0.0810, which corresponds well with both experimental red shift in absorption spectrum and strong orange color observed.[55,56]

The electronic parameters for the sensor and its complexes that were calculated are summarized in Fig. 8. The energy gap reduction trend is consistent with what happens when an analyte binds, which indicates that the sensing mechanism is energetically favorable and based on stable complex formation.

3.6 Sensing mechanism

The sensing performance of Phen-GA-MIL-53(Al) toward As^{3+} and Fe^{2+} is ultimately governed by the interplay between the hierarchical pore architecture of the host framework and the precisely engineered coordination environment of the anchored phenanthroline-glutaraldehyde assembly. Structural characterization by XRD confirms that the characteristic breathing channels of MIL-53(Al) remain fully accessible following post-synthetic modification, preserving unobstructed pathways for interfacial mass transfer. BET analysis further establishes that functionalization is concentrated within the internal pore

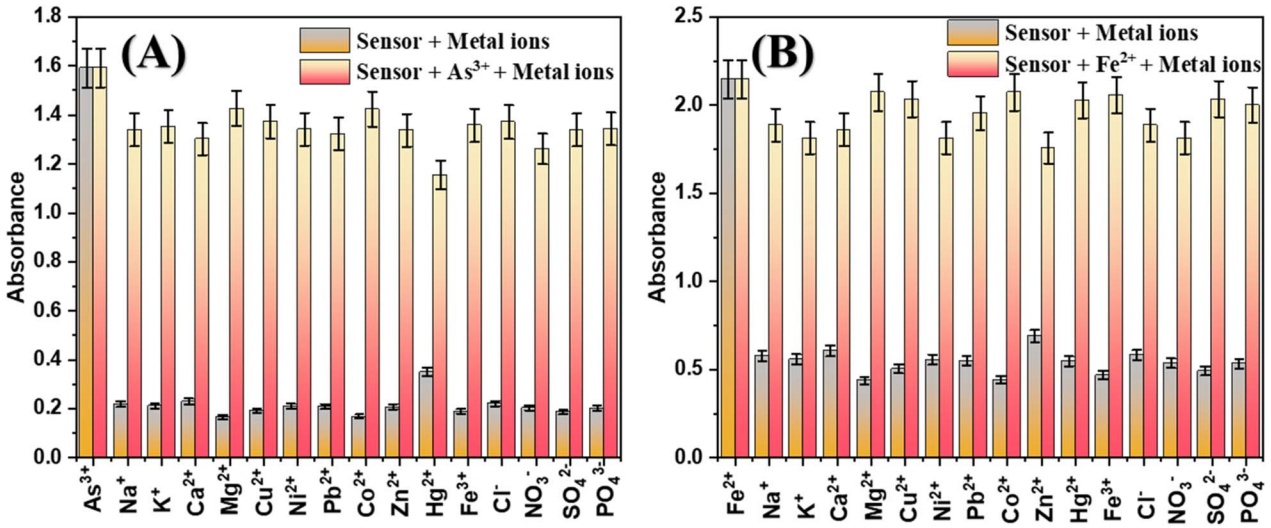

Fig. 7 Selectivity of the Phen-GA-MIL-53(Al) sensor towards As^{3+} and Fe^{2+} ions in the presence of various interfering ions.

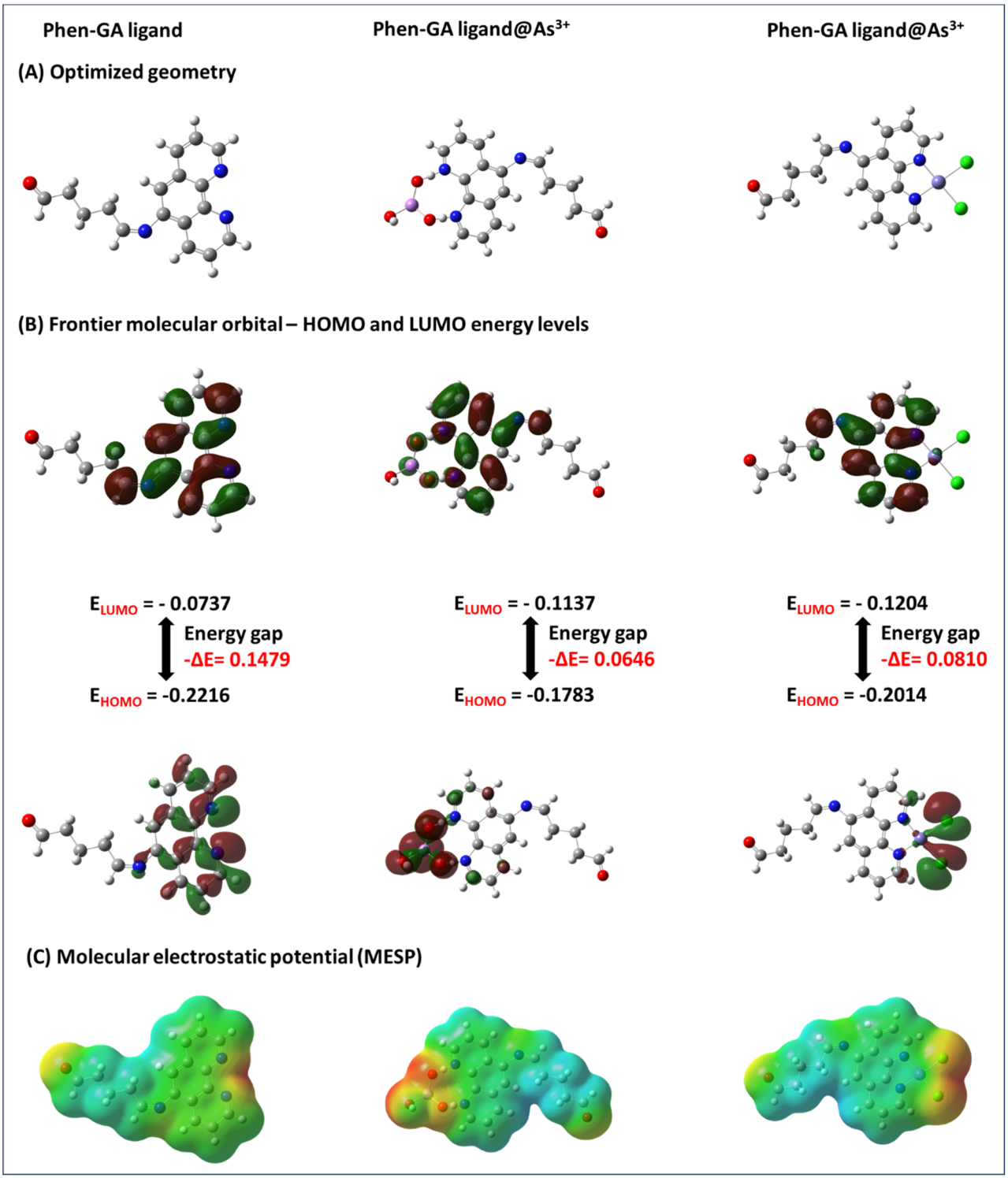

Fig. 8 (A) The optimized molecular geometries, (B) the frontier molecular orbital (FMO) analysis, and (C) the molecular electrostatic potential (MESP) maps for the Phen-GA ligand, Phen-GA ligand@As^{3+}, and Phen-GA ligand@Fe^{2+} complexes.

network ($S_{BET} = 1384\ m^2\ g^{-1}$), generating a confinement effect that locally elevates the density of active phenanthroline sites and accelerates analyte capture kinetics. The glutaraldehyde spacer is mechanistically indispensable in this regard: by decoupling the chelating head-group from the rigid Al–O secondary building units, it restores the conformational freedom required for multidentate coordination a flexibility that would otherwise be quenched by direct tethering to the inorganic nodes.

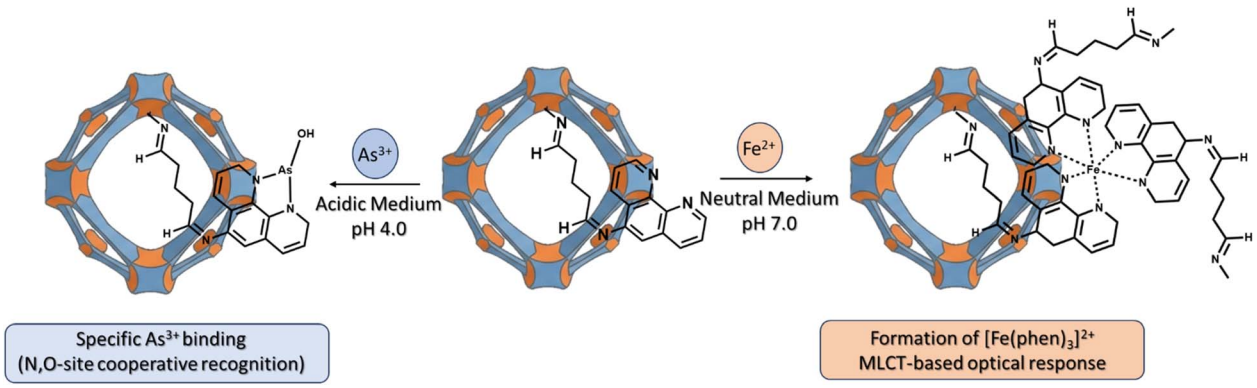

Scheme 2 Illustration of the dual-responsive sensing of Phen-GA-MIL-53(Al) toward As^{3+} and Fe^{2+} ions.

Against this structural backdrop, the two target analytes engage the sensing scaffold through fundamentally distinct but complementary recognition pathways. At pH 4.0, arsenic predominates as neutral arsenous acid, H_3AsO_3 ($pK_{a1} = 9.2$), a speciation that precludes simple electrostatic capture and instead engages a hydrogen-bond-mediated recognition protocol. The hydroxyl groups of H_3AsO_3 form an extensive network of intermolecular hydrogen bonds with the imine (C=N) and secondary amine (–NH_2) functionalities of the scaffold. Sequential binding order, resolved by 2D-COS FTIR asynchronous cross-peaks (Fig. 1E), reveals that the arsenic center first associates with the nitrogen-rich phenanthroline-imine sites before finding secondary stabilization through the oxygen-rich Al–carboxylate nodes a synergistic N,O-coordination mode that underpins the sensor's unusually high affinity for this metalloid relative to competing oxyanion species.[57]

Detection of Fe^{2+} proceeds by an electronically distinct mechanism. At pH 7.0, the fully deprotonated nitrogen donors of phenanthroline engage the Fe^{2+} center through strong covalent coordination, assembling the classical tris-chelate complex $[Fe(phen)_3]^{2+}$ within the MOF cavities. The immediate development of a characteristic orange-red coloration upon exposure confirms the formation of this complex, whose intense absorption arises from a metal-to-ligand charge transfer (MLCT) transition namely, electron density redistribution from the iron d-orbitals into the π^* manifold of the phenanthroline rings.

The thermodynamic stability of both complexes is independently corroborated by DFT calculations, which reveal a substantial contraction of the HOMO–LUMO energy gap (ΔE) upon analyte binding: from −0.1479 eV for the free ligand to −0.0646 eV for the As^{3+} complex and −0.0810 eV for the Fe^{2+} complex.[58,59] This narrowing of ΔE, accompanied by redistribution of HOMO electron density toward the bound metal center, confirms the formation of electronically coupled, chemically stable surface species rather than physisorbed aggregates.[60] SEM-EDX elemental mapping is fully consistent with this interpretation: arsenic and iron are distributed homogeneously across the framework surface (1.80 at% and 1.64 at%, respectively), with no evidence of localized clustering that would be indicative of non-specific adsorption.[61] This molecular-level dispersion of analyte across accessible coordination sites is, moreover, directly responsible for the sensor's high reusability, as it ensures that stripping agents thiourea and EDTA can efficiently access and regenerate sensing sites without inducing structural degradation of the framework (Scheme 2).[58]

3.7 Application

3.7.1 Determination of As^{3+} and Fe^{2+} ions in real water samples and dietary supplement. The analytical performance of

Table 3 Determination of As^{3+} and Fe^{2+} in spiked tap water samples and Dietary supplement using Br- Phen-GA-MIL-53(Al) sensor

			Proposed method		ICP-OES method	
Samples	Target ion	Added (ppb)	Found[a] (ppb)	Recovery (%)	Found[a] (ppb)	Recovery (%)
Tap water	As^{3+}	—	ND[b]	—	ND[b]	—
		50	49.57 ± 0.38	99.13	50.43 ± 0.12	100.87
		100	99.83 ± 0.21	99.83	100.37 ± 0.12	100.37
		200	198.70 ± 0.17	99.35	199.63 ± 0.12	99.82
Tap water	Fe^{2+}	—	38.63 ± 0.47	—	35.10 ± 0.10	—
		50	87.27 ± 0.31	97.27	85.13 ± 0.15	100.07
		100	137.63 ± 0.25	99.00	134.83 ± 0.15	99.73
		200	238.30 ± 0.20	99.83	234.90 ± 0.10	99.90
Dietary supplement		—	27.71 ± 0.35	—	29.07 ± 0.12	—

[a] Mean ± standard deviation ($n = 3$). [b] Not detected.

the developed Phen-GA-MIL-53(Al) sensor was assessed by determining As^{3+} and Fe^{2+} concentrations in different matrices, namely local tap water and a commercial dietary supplement. The accuracy of the proposed spectrophotometric method was verified using a standard addition protocol, and results were cross-validated with Inductively Coupled Plasma Optical Emission Spectroscopy (ICP-OES).

Table 3 presents a summary of the results obtained from the recovery studies. The pristine tap water sample analyzed showed that As^{3+} was not detected (ND). However, a trace background concentration of Fe^{2+} was found at 38.63 $\pm$ 0.47 ppb. In the dietary supplement sample analysis, Fe^{2+} was quantified at 27.71 $\pm$ 0.35 ppb.

After spiking the samples with known concentrations of As^{3+} and Fe^{2+} (50, 100, and 200 ppb), the Phen-GA-MIL-53(Al) sensor showed very good recovery rates between 97.27% and 99.83%. These figures are a testament to the sensor's high accuracy and its capacity to work well in the presence of different salts and minerals that are commonly found in municipal water or in dietary supplement without much interference.

The concentrations were determined by the proposed MOF-based method and were in excellent agreement with those obtained *via* ICP-OES Table 3. The relative errors were small, and the recovery percentages for both methods were statistically similar. This close correlation indicates that Phen-GA-MIL-53(Al) can be used as an inexpensive, portable substitute for high-tech laboratory equipment in trace metal analysis.

4. Conclusions

The article presents a novel and highly efficient dual-analyte spectrophotometric sensor, designated as Phen-GA-MIL-53(Al), which was developed through the covalent post-synthetic modification of an amino-functionalized aluminum-based metal–organic framework. This sensor used glutaraldehyde as a flexible molecular spacer and 5-amino-1,10-phenanthroline as the chromogenic recognition unit to create a robust sensing platform that can detect ultra-trace amounts of As^{3+} and Fe^{2+} in aqueous media. The XRD, BET, SEM-EDX, and FT-IR analyses carried out systematically confirmed that the structural integrity and hierarchical porosity of the MIL-53(Al) scaffold had been maintained. High resolution evidence for the sequential coordination involving nitrogen and oxygen donor sites was provided by 2D-COS FT-IR spectroscopy. Analytical results proved that this sensor works with exceptional sensitivity, achieving low detection limits. More specifically, a clear "naked-eye" chromogenic response was noted for Fe^{2+} in the sensor through an MLCT mechanism while As^{3+} would be quantified *via* a more advanced hydrogen-bonding and Lewis acid-base recognition pathway at acidic pH.

Theoretical validation through Density Functional Theory (DFT) confirmed results from experiments by showing a large decrease in the HOMO–LUMO energy gap with analyte binding. This change explains why there are spectrophotometric shifts. In addition, the sensor showed great selectivity toward common competing ions, maintained a stable shelf-life for up to six weeks, and demonstrated excellent reusability over six cycles with Thiourea and EDTA as regenerating agents. The Phen-GA-MIL-53(Al) sensor was practically tested in real samples, that is, tap water and dietary supplements, with recovery rates (97.27–99.83%) in very good agreement with the standard ICP-OES method. While the present work validates the sensor's efficacy in municipal water and dietary matrices, future research will focus on extending the application of Phen-GA-MIL-53(Al) to more chemically heterogeneous environments, such as seawater, industrial wastewater, and agricultural runoff. These studies will allow for a deeper exploration of the 'pore-size exclusion' and 'confinement effects' under extreme ionic strengths and varying redox potentials, further bridging the gap between advanced MOF-based nanomaterial synthesis and large-scale practical environmental remediation. In general, this work presents a versatile cost-effective strategy applicable in the field to carry out simultaneous monitoring of toxic metalloids and transition metals bridging advanced nanomaterial synthesis and practical environmental remediation.

Conflicts of interest

There are no conflicts to declare.

Data availability

Data for this article are available in the Zenodo repository at https://doi.org/10.5281/zenodo.20213930.

Acknowledgements

Princess Nourah bint Abdulrahman University Researchers Supporting Project number (PNURSP2026R122), Princess Nourah bint Abdulrahman University, Riyadh, Saudi Arabia.

References

1 G. I. Edo, P. O. Samuel, G. O. Oloni, G. O. Ezekiel, V. O. Ikpekoro, P. Obasohan, J. Ongulu, C. F. Otunuya, A. R. Opiti, R. S. Ajakaye, A. E. A. Essaghah and J. J. Agbo, Environmental persistence, bioaccumulation, and ecotoxicology of heavy metals, *Chem. Ecol.*, 2024, **40**, 322–349.

2 M. Sharma, R. Kant, A. K. Sharma and A. K. Sharma, Exploring the impact of heavy metals toxicity in the aquatic ecosystem, *Int. J. Energy Water Resour.*, 2025, **9**, 267–280.

3 H. Deng, Y. Tu, H. Wang, Z. Wang, Y. Li, L. Chai, W. Zhang and Z. Lin, Environmental behavior, human health effect, and pollution control of heavy metal(loid)s toward full life cycle processes, *Eco-Environ. Health*, 2022, **1**, 229–243.

4 Y. K. Mishra, A. Kaushik and A. Singh, Introduction to Advanced materials for sensing and biomedical applications, *Mater. Adv.*, 2024, **5**, 6346–6350.

5 P. P. Shreya, R. Jha, and S. Singh, *Advanced Semiconductor Sensing Technologies: Materials and Design Challenges at the Nanoscale, Semiconductor Nanoscale Devices: Materials and Design Challenges*, Bentham Science Publishers, 2025.

6 R. O. Ogunleye, S. Rusnáková, J. Javořík, M. Žaludek and B. Kotlánová, Advanced Sensors and Sensing Systems for Structural Health Monitoring in Aerospace Composites, *Adv. Eng. Mater.*, 2024, **26**, 2401745.
7 A. E. Noor, R. Fatima, S. Aslam, A. Hussain, Z. u. Nisa, M. Khan, A. A. A. Mohammed and M. Sillanpaa, Health risks assessment and source admeasurement of potentially dangerous heavy metals (Cu, Fe, and Ni) in rapidly growing urban settlement, *Environ. Res.*, 2024, **242**, 117736.
8 P. Babuji, S. Thirumalaisamy, K. Duraisamy and G. Periyasamy, Human Health Risks due to Exposure to Water Pollution: A Review, *Water*, 2023, 2532.
9 S. Y. Ganie, D. Javaid, Y. A. Hajam and M. S. Reshi, Arsenic toxicity: sources, pathophysiology and mechanism, *Toxicol. Res.*, 2024, **13**, tfad111.
10 H. Rahidul Hassan, A review on different arsenic removal techniques used for decontamination of drinking water, *Environ. Pollut. Bioavailab.*, 2023, **35**, 2165964.
11 M. Banaee, A. Zeidi, N. Mikušková and C. Faggio, Assessing Metal Toxicity on Crustaceans in Aquatic Ecosystems: A Comprehensive Review, *Biol. Trace Elem. Res.*, 2024, **202**, 5743–5761.
12 K. Jomova, S. Y. Alomar, E. Nepovimova, K. Kuca and M. Valko, Heavy metals: toxicity and human health effects, *Arch. Toxicol.*, 2025, **99**, 153–209.
13 B. K. Vinay, S. Bagchi and T. R. Suranjan, Chromium Detection in Water Using Optical Methods: A Study of Reagent and Reagentless Approaches, *Crit. Rev. Anal. Chem.*, 2026, **56**, 449–531.
14 S. Mohanty, G. Chowdary and S. G. Singh, Smartphone-powered portable chemiresistive sensing system for label free detection of lead ions in water, *Microchem. J.*, 2023, **194**, 109239.
15 S. Kashyap, S. Joshi, P. S. Mahan, S. Kayal and T. K. Mandal, A highly efficient indigenous portable optical sensor for measurement of total chromium concentration in environmental and biological samples: Design, development, and validation with spectroscopic results, *Microchem. J.*, 2025, **211**, 113098.
16 N. A. I. M. Mokhtar, R. M. Zawawi, W. M. Khairul and N. A. Yusof, Electrochemical and optical sensors made of composites of metal–organic frameworks and carbon-based materials. A review, *Environ. Chem. Lett.*, 2022, **20**, 3099–3131.
17 A. Das, S. Bej, N. R. Pandit, P. Banerjee and B. Biswas, Recent advancements of metal–organic frameworks in sensing platforms: relevance in the welfare of the environment and the medical sciences with regard to cancer and SARS-CoV-2, *J. Mater. Chem. A*, 2023, **11**, 6090–6128.
18 L. Zhang, G. Xiang, L. Zhang, R. Song, Y. Wang, Y. Mu and Z. Liu, Dual-functionalized MIL-53-NH_2 MOFs for high-capacity and reversible ammonia storage: Synergistic effects of hydrogen bonding and electrostatic interactions, *J. Environ. Chem. Eng.*, 2025, **13**, 118406.
19 B. Mohan, V. Virender, V. Pandey, I. M. Garazade, B. Najafov, X. Liao, A. J. L. Pombeiro, G. Singh and S. S. Kim, Fluorides Capture: Delving Into the Bond Between Metal–Organic Frameworks and Capture Dynamics, *Adv. Sustain. Syst.*, 2025, **9**, e00304.
20 S. Pandey and S. Mishra, A review of sensing technologies for arsenic detection in drinking water, *Int. J. Environ. Sci. Technol.*, 2025, **22**, 2809–2832.
21 T. Gadzikwa and P. Matseketsa, The post-synthesis modification (PSM) of MOFs for catalysis, *Dalton Trans.*, 2024, **53**, 7659–7668.
22 A. Enriquez-Cabrera, L. Getzner, L. Salmon, L. Routaboul and A. Bousseksou, Post-synthetic modification mechanism for 1D spin crossover coordination polymers, *New J. Chem.*, 2022, **46**, 22004–22012.
23 Y. Lai, A. Enríquez-Cabrera, A. Ronci, L. Salmon, L. Routaboul and A. Bousseksou, When the Study of the Post-Synthetic Modification Method on a 1D Spin Crossover Coordination Polymer Highlights its Catalytic Activity, *Chem.–Eur. J.*, 2025, **31**, e202403412.
24 X. Lu, K. Jayakumar, Y. Wen, A. Hojjati-Najafabadi, X. Duan and J. Xu, Recent advances in metal-organic framework (MOF)-based agricultural sensors for metal ions: a review, *Microchim. Acta*, 2023, **191**, 58.
25 S. C. Pal, D. Mukherjee and M. C. Das, pH-Stable Luminescent Metal–Organic Frameworks for the Selective Detection of Aqueous-Phase FeIII and CrVI Ions, *Inorg. Chem.*, 2022, **61**, 12396–12405.
26 L. Zhang, J. Wang, T. Du, W. Zhang, W. Zhu, C. Yang, T. Yue, J. Sun, T. Li and J. Wang, NH2-MIL-53 (Al) metal–organic framework as the smart platform for simultaneous high-performance detection and removal of Hg2+, *Inorg. Chem.*, 2019, **58**, 12573–12581.
27 J. Hafizovic, M. Bjørgen, U. Olsbye, P. D. Dietzel, S. Bordiga, C. Prestipino, C. Lamberti and K. P. Lillerud, The inconsistency in adsorption properties and powder XRD data of MOF-5 is rationalized by framework interpenetration and the presence of organic and inorganic species in the nanocavities, *J. Am. Chem. Soc.*, 2007, **129**, 3612–3620.
28 D. Saha and S. Deng, Structural stability of metal organic framework MOF-177, *J. Phys. Chem. Lett.*, 2010, **1**, 73–78.
29 J. Kim, D. O. Kim, D. W. Kim and K. Sagong, Synthesis of MOF having hydroxyl functional side groups and optimization of activation process for the maximization of its BET surface area, *J. Solid State Chem.*, 2013, **197**, 261–265.
30 H. Mao, J. Xu, Y. Hu, Y. Huang and Y. Song, The effect of high external pressure on the structure and stability of MOF α-Mg 3 (HCOO) 6 probed by in situ Raman and FT-IR spectroscopy, *J. Mater. Chem. A*, 2015, **3**, 11976–11984.
31 G. Kumar, R. Haldar, M. Shanmugam and R. S. Dey, Mechanistic insight into a Co-based metal–organic framework as an efficient oxygen electrocatalyst via an in situ FT-IR study, *J. Mater. Chem. A*, 2023, **11**, 26508–26518.
32 P. Musto, P. La Manna, M. Pannico, G. Mensitieri, N. Gargiulo and D. Caputo, Molecular interactions of CO2 with the CuBTC metal organic framework: An FTIR study based on two-dimensional correlation spectroscopy, *J. Mol. Struct.*, 2018, **1166**, 326–333.

33 J. Nishida, A. Tamimi, H. Fei, S. Pullen, S. Ott, S. M. Cohen and M. D. Fayer, Structural dynamics inside a functionalized metal–organic framework probed by ultrafast 2D IR spectroscopy, *Proc. Natl. Acad. Sci. U. S. A.*, 2014, **111**, 18442–18447.

34 S. Halder, J. Mondal, J. Ortega-Castro, A. Frontera and P. Roy, A Ni-based MOF for selective detection and removal of Hg 2+ in aqueous medium: a facile strategy, *Dalton Trans.*, 2017, **46**, 1943–1950.

35 P. Sanati-Tirgan, H. Eshghi and A. Mohammadinezhad, Designing a new method for growing metal–organic framework (MOF) on MOF: synthesis, characterization and catalytic applications, *Nanoscale*, 2023, **15**, 4917–4931.

36 C. Petit and T. J. Bandosz, MOF–graphite oxide composites: combining the uniqueness of graphene layers and metal–organic frameworks, *Adv. Mater.*, 2009, **21**, 4753–4757.

37 P. Hirschle, T. Preiß, F. Auras, A. Pick, J. Völkner, D. Valdepérez, G. Witte, W. J. Parak, J. O. Rädler and S. Wuttke, Exploration of MOF nanoparticle sizes using various physical characterization methods–is what you measure what you get?, *CrystEngComm*, 2016, **18**, 4359–4368.

38 B. Chen, X. Wang, Q. Zhang, X. Xi, J. Cai, H. Qi, S. Shi, J. Wang, D. Yuan and M. Fang, Synthesis and characterization of the interpenetrated MOF-5, *J. Mater. Chem.*, 2010, **20**, 3758–3767.

39 H. Li, W. Shi, K. Zhao, H. Li, Y. Bing and P. Cheng, Enhanced hydrostability in Ni-doped MOF-5, *Inorg. Chem.*, 2012, **51**, 9200–9207.

40 H. M. Abumelha, N. M. Alourfi, A. S. Al Zbedy, A. Alharbi, N. Alkhathami, I. Mousa, M. A. Khalil and N. M. El-Metwaly, Functionalized cellulose nanomaterials as a fluorescent 'turn-off' sensor for Ag+ ions in aqueous solutions and pharmaceutical samples, *J. Water Proc. Eng.*, 2025, **77**, 108381.

41 N. Y. Elamin, M. R. Elamin, S. Abdalla, M. A. Khalil, A. A. Helaly, B. A. Babgi and M. A. Hussien, Bioengineered nanocellulose–Schiff base sensor for selective fluorometric detection of Cd2+ ions in aqueous media, *Int. J. Biol. Macromol.*, 2025, **328**, 147594.

42 S. Nagarani, J.-H. Chang, M. Yuvaraj, S. Balachandran, M. Kumar and S. Kanimozhi, Well-organized metal-free chemically reduced graphene oxide sheets as electrocatalysts for enhanced oxygen reduction reactions in alkaline media, *Mater. Lett.*, 2024, **357**, 135705.

43 R. Dhilip Kumar, A. J. Kumar, S. Balachandran, F. V. Kusmartsev, A. B. G. Trabelsi, F. H. Alkallas, S. Nagarani, V. Sethuraman and B.-K. Lee, High-performance chrysanthemum flower-like structure of Ni doped ZnO nanoflowers for pseudo-supercapacitors, *J. Energy Storage*, 2023, **72**, 108441.

44 K. Deepa and Y. Lingappa, A simple spectrophotometric method for the determination of arsenic in industrial and environmental samples using 2,4-Dihydroxy benzophenone-2-amino thiophenol, *Spectrochim. Acta, Part A*, 2014, **124**, 102–107.

45 S. d. F. P. Pereira, S. L. C. Ferreira, G. Oliveira, D. d. C. Palheta and B. Barros, Spectrophotometric determination of arsenic in soil samples using 2-(5-bromo-2-pyridylazo)-5-di-ethylaminophenol (Br-PADAP), *Eclét. Quím.*, 2008, **33**, 23–28.

46 T. Cherian and B. Narayana, A new spectrophotometric method for the determination of arsenic in environmental and biological samples, *Anal. Lett.*, 2005, **38**, 2207–2216.

47 H. Revanasiddappa, B. Dayananda and T. Kumar, A sensitive spectrophotometric method for the determination of arsenic in environmental samples, *Environ. Chem. Lett.*, 2007, **5**, 151–155.

48 S. Lu, X. Zhang, L. Chen and P. Yang, Colorimetric determination of ferrous ion via morphology transition of gold nanorods, *Microchim. Acta*, 2018, **185**, 76.

49 M. J. Ahmed and U. K. Roy, A simple spectrophotometric method for the determination of iron (II) aqueous solutions, *Turk. J. Chem.*, 2009, **33**, 709–726.

50 D. Ondigo, Z. Tshentu and N. Torto, Electrospun nanofiber based colorimetric probe for rapid detection of Fe2+ in water, *Anal. Chim. Acta*, 2013, **804**, 228–234.

51 K. Zheng, C. Lai, L. He and F. Li, Chromo-chemodosimetric detection for Fe2+ by Fenton reagent-induced chromophore-decolorizing of halogenated phenolsulfonphthalein derivatives, *Sci. China Chem.*, 2010, **53**, 1398–1405.

52 A. M. John, J. Jose, R. Thomas, K. J. Thomas and S. P. Balakrishnan, Spectroscopic and TDDFT investigation of highly selective fluoride sensors by substituted acyl hydrazones, *Spectrochim. Acta, Part A*, 2020, **236**, 118329.

53 E. I. Edache, A. Uzairu, P. A. Mamza, G. A. Shallangwa and M. T. Ibrahim, DFT studies on structure, electronics, bonding nature, NBO analysis, thermodynamic properties, molecular docking, and MM-GBSA evaluation of 4-methyl-3-[2-(4-nitrophenyl)-1, 3-dioxo-2, 3-dihydro-1 H-isoindole-5-amido] benzoic acid: a potent inhibitor of Graves' disease, *J. Umm Al-Qura Univ. Appl. Sci.*, 2024, 1–19.

54 W. Abd El-Fattah, A. Guesmi, N. Ben Hamadi, M. A. Khalil, A. A. Helaly, B. A. Babgi and M. A. Hussien, Eco-friendly spectrophotometric sensor based on Schiff-base functionalized cellulosic material for ultra-sensitive mercury(II) detection, *Microchem. J.*, 2025, **218**, 115380.

55 W. Kohn, A. D. Becke and R. G. Parr, Density functional theory of electronic structure, *J. Phys. Chem.*, 1996, **100**, 12974–12980.

56 T. A. Fayed, M. Gaber, G. M. Abu El-Reash and M. M. El-Gamil, Structural, DFT/B3LYP and molecular docking studies of binuclear thiosemicarbazide Copper (II) complexes and their biological investigations, *Appl. Organomet. Chem.*, 2020, **34**, e5800.

57 A. Subhasri, S. Balachandran, M. Chandrakanth, S. Sowmiya, S. Vasugi, S. Devanesan and M. S. AlSalhi, Design, synthesis, and selective sensing of Sr2+ ions using fluorescent aryl acetamide sensors with computational and biological investigations, *J. Mol. Struct.*, 2025, **1333**, 141739.

58 B. Subramanian, J. J. Kumaravel, R. Rajendran, R. Duraisamy, D. K. Rajaiah, N. Sandhiran, R. Govindasamy, S. Pandiaraj, M. Rahaman and J.-H. Chang, Hydrothermal fabrication of two-dimensional

indium oxide nanosheets for high-performance supercapacitors, *Mater. Lett.*, 2024, **358**, 135835.

59 S. Balachandran, K. J. Jothi, S. Muthamizh, A. Subhasri, R. D. Kumar, A. S. K. Kumar, M. A. Wadaan and H. Chengzhi, Facile fabrication of BiVO4 Microspheres: Investigating their twin application on potential in electrochemical capacitors and protein detection, *J. Power Sources*, 2025, **650**, 237481.

60 R. B. Shivani, J. Mani, J. Balachandran, J. Kasthuri and R. Mohan Kumar, Intercalation of Bi2S3–graphene into MXene nanosheets: a novel strategy for enhanced thermoelectric performance, *J. Mater. Sci.: Mater. Electron.*, 2025, **36**, 1371.

61 G. Anbalagan, Z. Xu, J. J. Kumaravel, V. Suresh, B. Subramanian, N. Sandhiran, S. Devanesan, M. S. AlSalhi and M. Yang, Hydrothermal synthesis of InVO4/Bi2S3 heterojunctions for enhanced efficiency in visible-light photocatalysis and hydrogen evolution reactions, *J. Power Sources*, 2025, **647**, 237346.